Lockheed

HUNTSVILLE RESEARCH & ENGINEERING CENTER

LOCKHEED MISSILES & SPACE COMPANY, INC.
A SUBSIDIARY OF LOCKHEED AIRCRAFT CORPORATION

HUNTSVILLE, ALABAMA

HREC-0515-6
LMSC-HREC D225642-I

LOCKHEED MISSILES & SPACE COMPANY
HUNTSVILLE RESEARCH & ENGINEERING CENTER
HUNTSVILLE RESEARCH PARK
4800 BRADFORD DRIVE, HUNTSVILLE, ALABAMA

CONTROL SYSTEM OPTIMIZATION STUDIES

FINAL REPORT

VOLUME I

PAYLOAD DEPLOYMENT STUDY

March 1972

Contract NAS8-30515
(Appendix F)

Prepared for National Aeronautics and Space Administration
Marshall Space Flight Center, Alabama 35812

by

G.M. Heeschen
A.M. Hansing

APPROVED: W. Trautwein

W. Trautwein, Supervisor
Flight Dynamics & Control Section

T.R. Beal

T. R. Beal, Manager
Dynamics & Guidance Dept.

J.S. Farrior

J.S. Farrior
Resident Director

FOREWORD

This report presents results of the fourth in a series of studies to analyze earth orbital maneuvers including stationkeeping and docking. The work was performed by Lockheed's Huntsville Research & Engineering Center for NASA-Marshall Space Flight Center under Contract NAS8-30515. The three previous studies are documented in References 1, 2 and 3.

The present study was performed during the period 1 July 1971 to 6 March 1972 in accordance with Modification 9 of Appendix F. A second independent study — "High Frequency Cutoff Filter Analysis," was completed under this same contract and is documented in Volume II.

The NASA-MSFC technical coordinators for the study were Mr. E. C. Smith and Mr. M. Brooks of S&E-ASTR-SG.

CONTENTS

Section 1
INTRODUCTION AND SUMMARY

Many space missions planned for the future will require orbiting space vehicles to maneuver in close proximity (less than 1000 meters) to each other. Mission tasks requiring such maneuvers include stationkeeping, docking, orbital assembly, satellite inspection and retrieval, and payload deployment. Before a system is designed to perform these tasks, the critical parameters must be defined and alternative concepts investigated. Some major variables include mass and inertia properties, vehicle geometry, sensor data (amount and accuracy), reaction control system sophistication and manual involvement in the control loop.

During this study a simulation capability was developed to evaluate the alternative methods and hardware proposed to accomplish the tasks described. The fixed base simulation is performed on a hybrid computer, and includes a cathode ray tube display so that the maneuvers can be visually monitored by a pilot located in the active vehicle. Both automatic and manual control modes are included and the pilot can switch between these two modes at his discretion. Major simulation components which were developed in previous studies are: (1) Equations for generating the CRT display (Ref. 1); (2) two-burn translation logic for automatic docking (Ref. 2); and (3) baseline automatic attitude control system (Ref. 3).

A complete description of the hybrid simulation is presented in Section 2, and simulation results are described in Section 3. Major digital subroutines are described and flow charted in Appendix A, and the analog wiring diagrams are presented in Appendix B.

Section 2
PROGRAM DESCRIPTION

2.1 GENERAL DISCUSSION

The hybrid computer program developed during this study simulates the motion of a chase vehicle as it maneuvers for stationkeeping, inspection, or docking relative to a target vehicle. A typical docking situation is illustrated in Fig. 2-1. The target vehicle is assumed moving in a circular earth orbit with its attitude fixed relative to some reference axis (either the local vertical coordinates pictured or an inertial frame). Chaser six-degree-of-freedom motion is controlled with attitude and translation reaction control

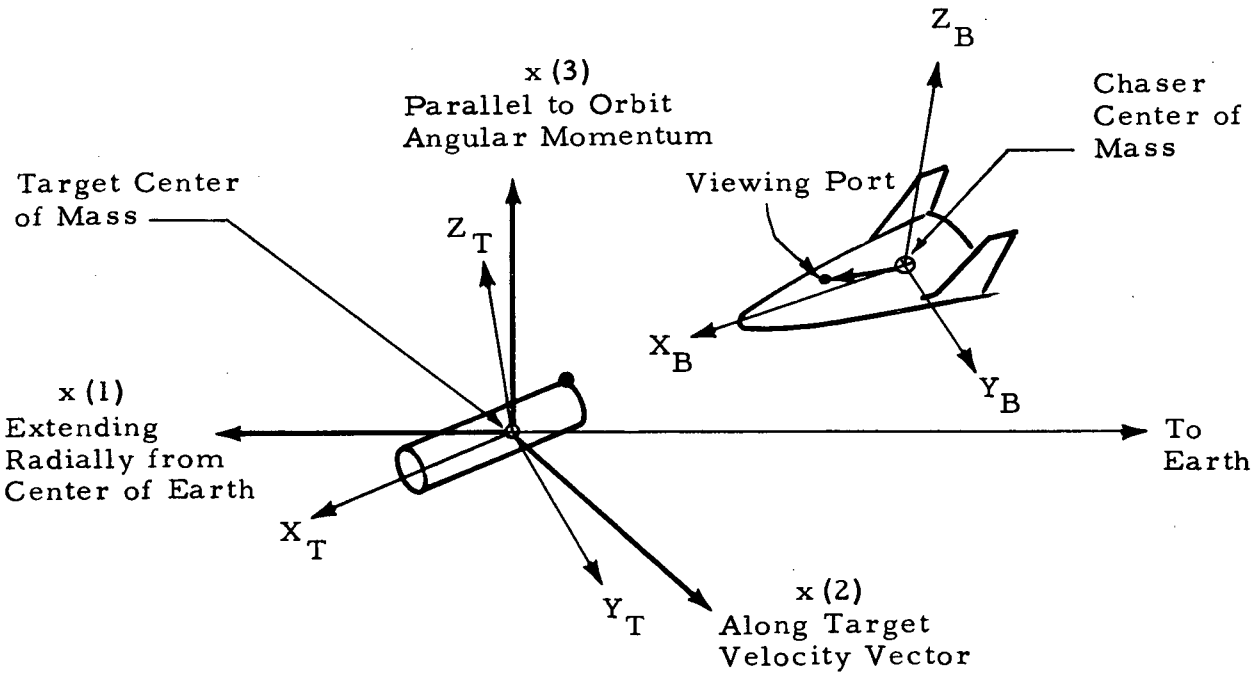

Fig. 2-1 - Typical Docking Situation

thrusters and is disturbed by gravity gradient torques. Translation and attitude maneuvers are limited by analog scaling as follows:

Maximum Range	= 1000 meters
Minimum Range	= Precontact
Maximum Velocity	= 5.0 meters/second
Maximum Angular Rate	= 0.1 radians/second

Five major program options are listed below.

1. Chaser Control Mode
   - Automatic
   - Manual
   - Real time switching between automatic and manual control at the pilot's discretion.

2. Target Attitude
   - Local vertical hold
   - Inertial hold

3. Sensor Accuracy
   - Perfect sensors
   - Effect of sensor inaccuracies introduced through measureables

4. Application of Control Forces
   - Applied along body axes
   - Applied along local vertical axes
   - Set identically equal to zero

5. Automatic Control Torques
   - From baseline attitude control laws
   - Set identically equal to zero.

Computer runs involving pilot interaction (manual and switching control modes) must be made in real time. Runs which use purely automatic control, however, can be made at accelerated run speeds (currently 10 times real time) to achieve a savings in computer time.

Figure 2-2 is a block diagram which shows the major elements of the hybrid simulation. This figure also shows how the work load is distributed between pilot, digital computer, and analog computer. Sections 2.2 — 2.6 further describe the program operation and capabilities. A summary of results is presented in Section 3.

Major digital subroutines are described and flow charted in Appendix A, and the analog wiring diagrams are documented in Appendix B.

2.2 TARGET DISPLAY AND DOCKING CONDITIONS

A representation of the target vehicle is generated on a CRT display scope for visual feedback to the pilot. In the present display the target is represented by a cylinder. A bright spot on one of the cylinder end circles represents a docking target and defines the front face. Clues as to the relative target attitude are obtained from spot location, direction of the cylinder centerline, flattening of the end circles, and relative size of the end circles. The overall display size gives range information. The pilot attempts to fly into the cylinder front face along the cylinder centerline which is assumed to be the docking axis. The angular field of view displayed on the scope is a program input called α_F. All display elements are normalized by α_F before positioning on the screen.

Figure 2-3 illustrates the cylindrical representation of the target. RHOZM, RHOZP and RADIUS are program inputs. During the simulation the target holds a constant input attitude relative to some reference frame (inertial or local vertical) as shown in Fig. 2-4. Normally, during checkout runs the target is kept aligned with the local vertical coordinates so that the docking axis ($-X_T$) is directed toward the earth. The chase vehicle is considered docked, and the run terminated automatically when the range to the target front face is less than some input value, PM1.

During periods of automatic control the chase vehicle translates to a rendezvous point located along the docking axis and defined by the input variable PM2. When PM2 is greater than PM1, docking can only be completed

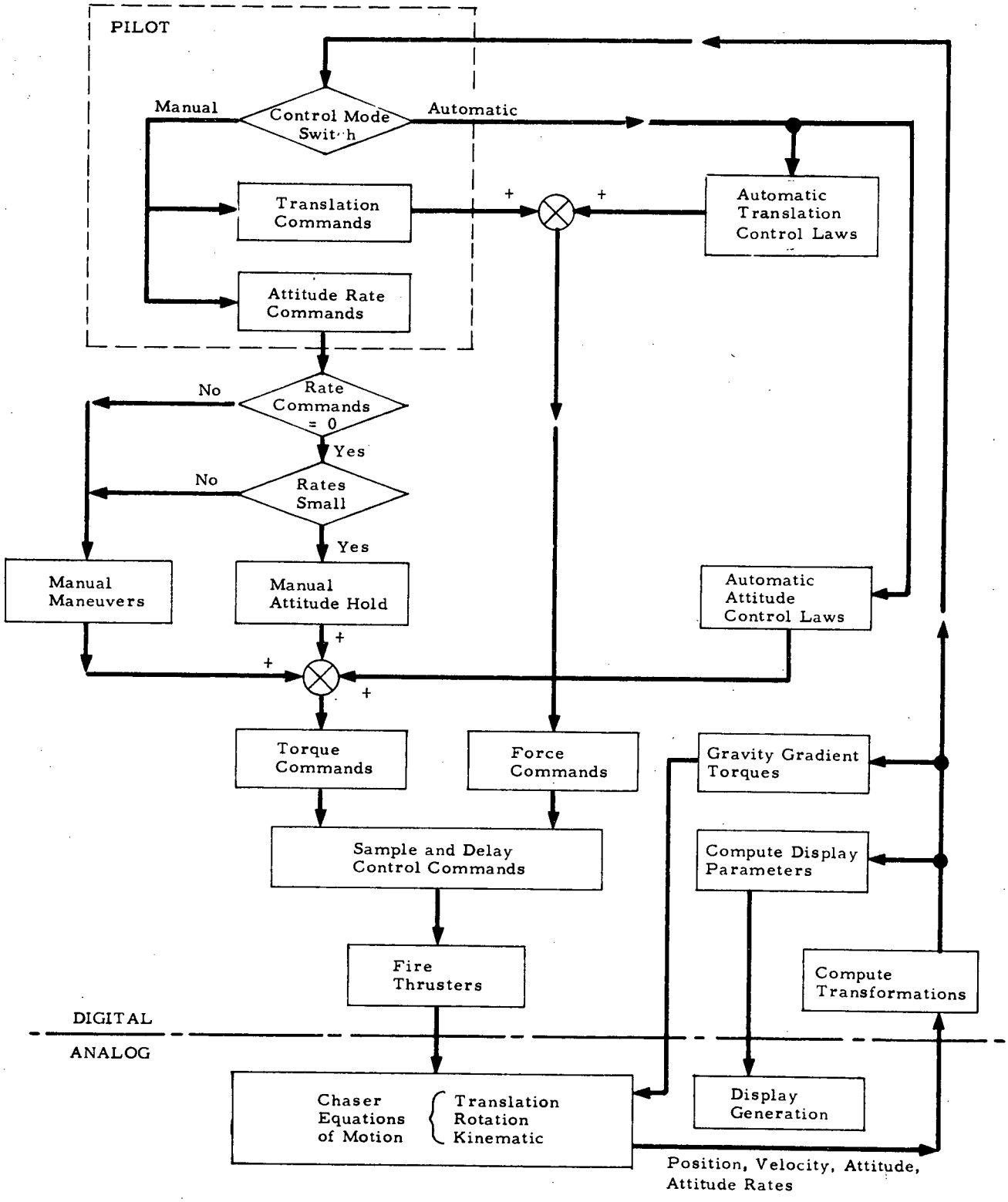

Fig. 2-2 - Block Diagram of Hybrid Docking Simulation

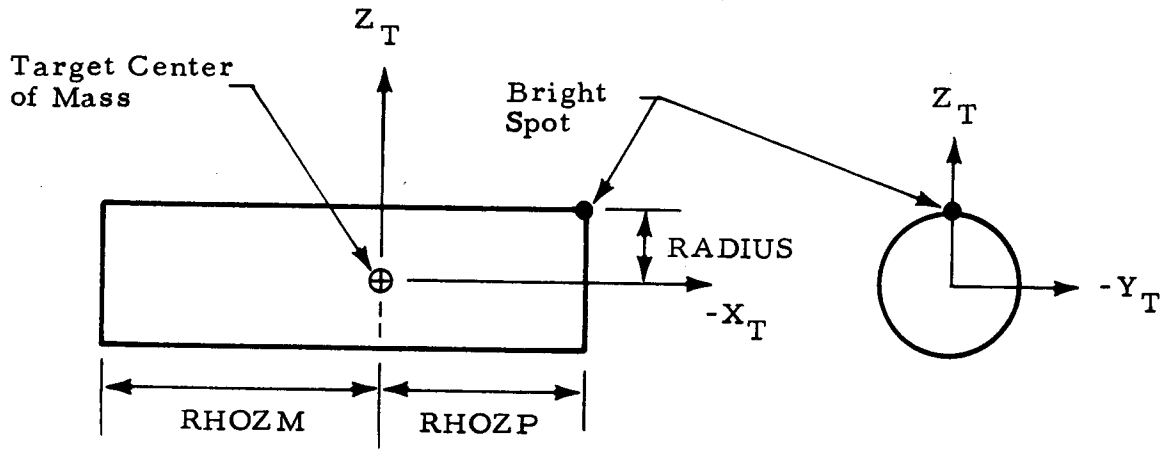

Fig. 2-3 - Cylindrical Representation of Docking Target

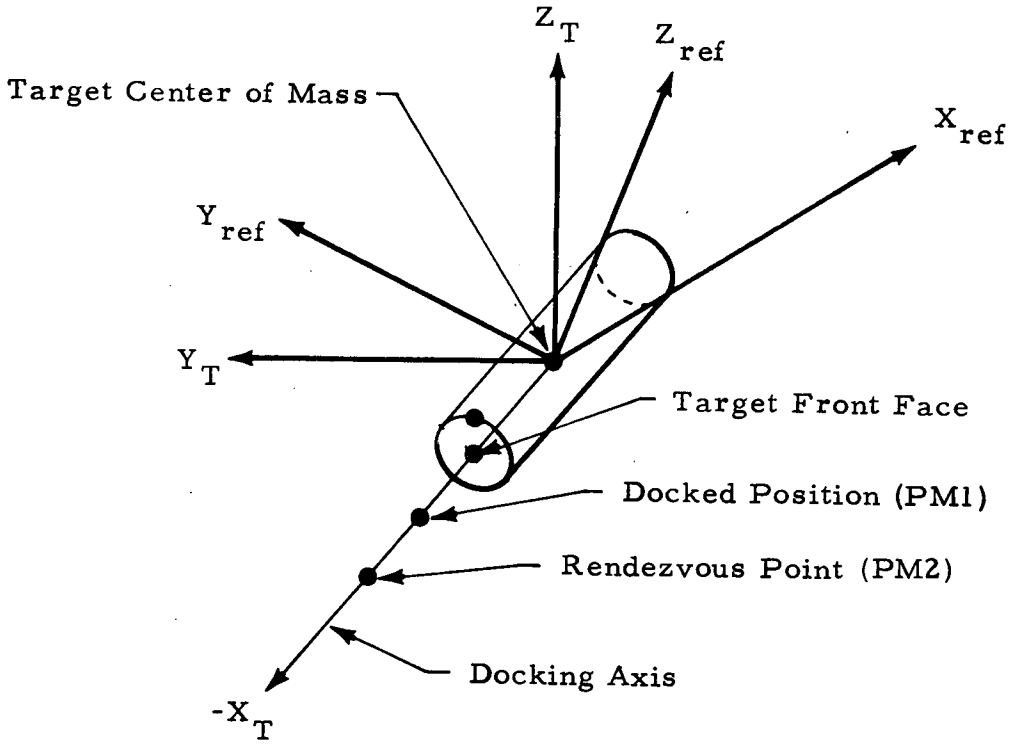

Fig. 2-4 - Docking Geometry

by switching to manual control. Nominal data for the target display and docking conditions is shown in Table 2-1. The input value for α_F was computed as follows so that after a perfect dock the target front face will just fill the CRT display scope.

$$\alpha_F = \tan^{-1} \frac{\text{RADIUS}}{\text{PM1}}$$

Table 2-1
NOMINAL TARGET AND DOCKING DATA

Input Name	Nominal Value
RHOZM	5.0 m
RHOZP	5.0 m
RADIUS	3.0 m
PM1	1.732 m
PM2	2.0 m
ALFAF (α_F)	1.05 rad

2.3 CHASE VEHICLE EQUATIONS OF MOTION

The chaser equations of motion are solved on the analog computer. These equations are described briefly below and the detailed wiring diagrams are shown in Appendix B.

● Translation Equations — The translation equations are solved in local vertical coordinates and were derived by Clohessy and Wiltshire (Aerospace Science, September 1960).

$$\ddot{x}(1) = \frac{1}{m} F_1 + 2\omega\dot{x}(2) + 3\omega^2 x(1)$$

$$\ddot{x}(2) = \frac{1}{m} F_2 - 2\omega\dot{x}(1)$$

$$\ddot{x}(3) = \frac{1}{m} F_3 - \omega^2 x(3)$$

The terms x(1), x(2) and x(3) are the local vertical coordinates defined in Fig. 2-1. The F_i are control forces, m is the chaser mass, and ω is the target orbital rate in radians per second. A dot above a variable indicates differentiation with respect to time. The cross-coupling terms which are all a function of ω can be removed from the simulation with a simple switch.

● Rotational Equations — Body angular rates (P, Q and R) are computed as shown below. Note that body axes are assumed to be principal axes.

$$I_{xx}\dot{P} + (I_{zz} - I_{yy})\,QR = TC_x + TG_x$$

$$I_{yy}\dot{Q} + (I_{xx} - I_{zz})\,PR = TC_y + TG_y$$

$$I_{zz}\dot{R} + (I_{yy} - I_{xx})\,PQ = TC_z + TG_z$$

Control torques, TC, and gravity gradient torques, TG, are computed on the digital and sent to the analog separately to facilitate scaling.

● Kinematic Equations — The chaser attitude is computed by integrating a set of four Euler parameters which relate body axes to inertial axes. These equations have no singularities so that all attitudes can be simulated. Orthogonality is assured by forcing the sum of the squares to equal one. This is all done continuously on the analog.

Nominal values for chaser mass properties, control forces, and control torques are shown below.

Chaser Parameter	Nominal Value
Mass	1.264×10^5 kg
I_{xx}	4.203×10^6 kg-m^2
I_{yy}	2.052×10^7 kg-m^2
I_{zz}	2.319×10^7 kg-m^2
F_i	7.340×10^3 N
TC_x	2.712×10^4 N-m
TC_y	5.762×10^4 N-m
TC_z	5.084×10^4 N-m

2.4 AUTOMATIC CONTROL

The control laws for attitude control during automatic docking were developed and incorporated into the simulation during a previous study (Ref. 3). These control laws are sub-optimal when the minimum impulse bit is one-third of the digital sampling interval, but they do not include the effects of system time delays. When the automatic and manual modes were combined to permit switching, a 0.14 second system time delay was introduced into the automatic mode. This was necessary to ensure compatability between automatic and manual control. The time delay caused rate overshoot during the elimination of attitude errors and also introduced limit cycle behavior while the chaser was in attitude hold.

This problem was remedied without sacrificing system accuracy by compensating for the time delay in the control logic. Figure 2-5 shows time histories of the chaser angular accelerations and angular rates with and without the control law modifications. These runs were initialized with a 10-degree attitude error about each of the chaser axes. The cause of instability and the control law modifications required to eliminate it are discussed below.

The optimum switching lines derived in Ref. 3 are valid for only a very restricted number of inputs. Two categories of imperfection may arise:

1. Errors, miscalculations, and finite time delays in the computing elements required to generate the optimum switching line, sense the state of the system, and switch the torque at the proper instant.

2. The effects of system inputs or loads other than those used to derive the optimum switching line.

These imperfections will cause slightly nonoptimum switching which, in turn, may permit the state of the system to overtravel the switching line, reverse, overtravel again, and so forth. The system state then approaches equilibrium while executing a high frequency oscillation in the vicinity of the switching line. As an example, the effect of time delay is shown in Fig. 2-6. In this

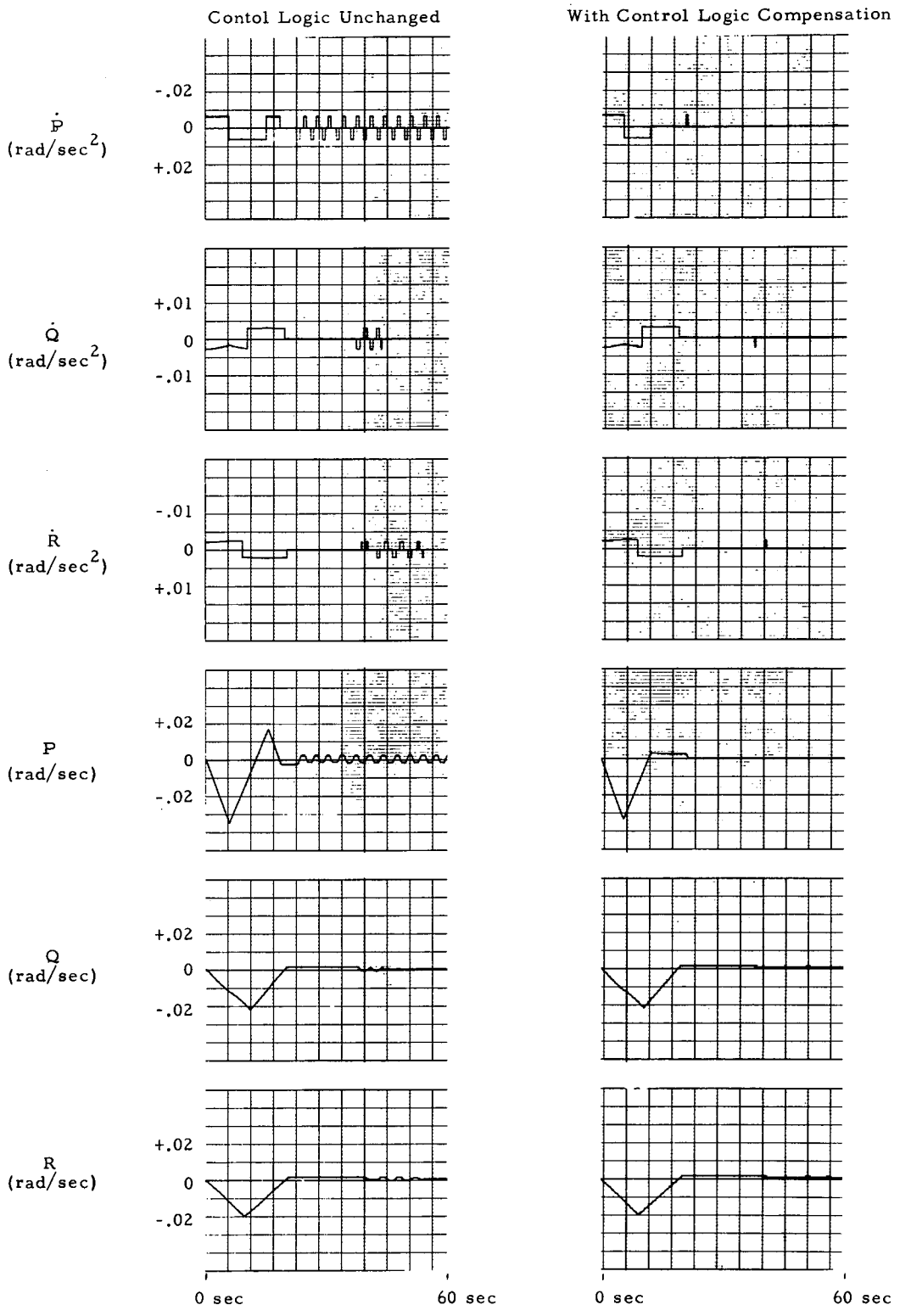

Fig. 2-5 - Chaser Angular Accelerations and Angular Velocities Versus Time During the Elimination of 10° Attitude Errors and with a 0.14 Second System Time Delay

case the actual switching line is a parabola of the same shape as the optimum (commanded) switching line but displaced from it in both the E and $\dot{E}$ directions. From this example we see that late switching caused by system time delays will produce wasteful firings by the control system.

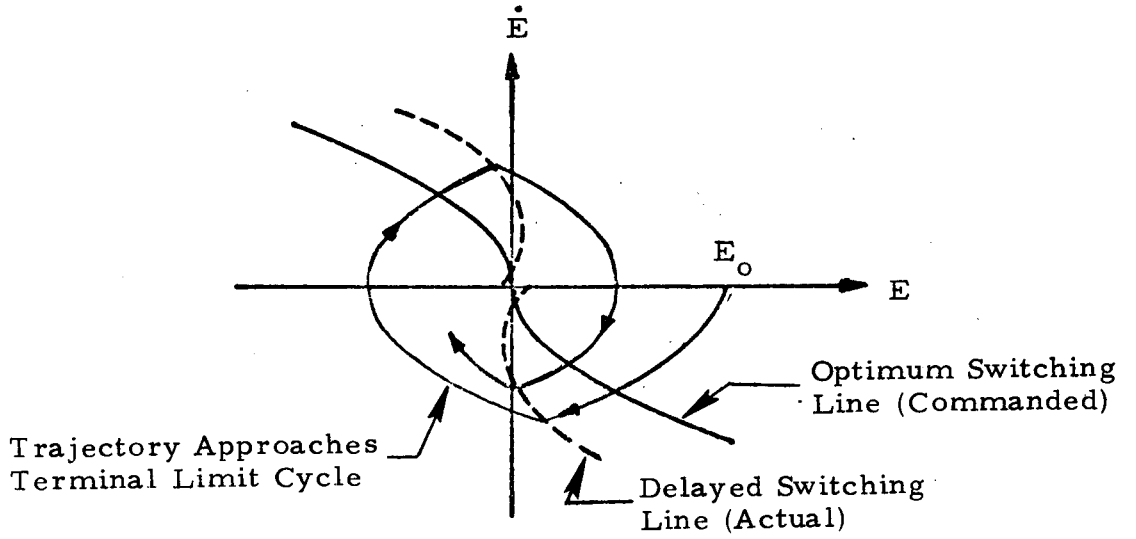

Fig. 2-6 - Phase Plane Description of How System Time Delays Affect the Control Logic Switching

The equation of the parabolic trajectory in the lower half plane following a step input is

$$\dot{E}^2 = -\frac{2L}{I}(E - E_o)$$

where I and L are the moment of inertia and torque about the axis of interest and E_o is the initial error. In the phase plane $\dot{E} = dE/dt$ or $dt = dE/\dot{E}$. Therefore, in the lower half plane,

$$t = \int_{E_o}^{E} \frac{dE}{\dot{E}} = \sqrt{-\frac{2I}{L}(E - E_o)}$$

and we can express E and $\dot{E}$ as follows:

$$E = -\frac{Lt^2}{2I} + E_o$$

$$\dot{E} = -\frac{Lt}{I}$$

If we use the subscript sw to denote system conditions at the switching point, the switching line can be expressed as:

$$E_{sw} = \frac{I}{2L}(\dot{E}_{sw})^2 \qquad (1)$$

also

$$E_{sw} = -\frac{L}{2I}(t_{sw})^2 + E_o$$

$$\dot{E}_{sw} = -\frac{Lt_{sw}}{I}$$

Now the time at which the torque reversal actually takes place is delayed beyond the time t_{sw}, by the time delay, τ, so that the delayed switching line occurs at

$$\dot{E}'_{sw} = -\frac{Lt'_{sw}}{I} = \dot{E}_{sw} - \frac{L\tau}{I}$$

$$E'_{sw} = -\frac{L(t'_{sw})^2}{2I} + E_o = E_{sw} + (\dot{E}'_{sw})\tau + \frac{L\tau^2}{2I}$$

or

$$\dot{E}_{sw} = \dot{E}'_{sw} + \frac{L\tau}{I}$$

$$E_{sw} = E'_{sw} - \left[(\dot{E}'_{sw})\tau + \frac{L\tau^2}{2I}\right]$$

Substituting into Eq. (1)

$$E'_{sw} - \left[(\dot{E}'_{sw})\tau + \frac{L\tau^2}{2I}\right] = \frac{I}{2L}\left[\dot{E}'_{sw} + \frac{L\tau}{I}\right]^2$$

rearranging, we get

$$E'_{sw} + \frac{L\tau^2}{I} = \frac{I}{2L}\left[\dot{E}'_{sw} + \frac{2L\tau}{I}\right]^2$$

This is the trajectory of the lower delayed switching line — with apex occurring $E'_{sw} = -L\tau^2/2$ and $\dot{E}'_{sw} = -2L\tau/I$. Similarly, the trajectory of the upper delayed switching line is

$$E'_{sw} - \frac{L\tau}{I} = -\frac{I}{2L}\left[\dot{E}'_{sw} - \frac{2L\tau}{I}\right]^2$$

Its apex occurs at $E'_{sw} = -L\tau^2/2$ and $\dot{E}'_{sw} = 2L\tau/I$.

The original optimum switching lines were designed for zero time delay. In order to compensate for the effect of a constant time delay, it was necessary to advance the switching time by an amount exactly equal to the time delay. We now let t''_{sw} be an advanced switching time which occurs τ seconds prior to t_{sw}. Then the advanced switching line occurs at

$$\dot{E}''_{sw} = -\frac{L(t''_{sw})}{I} = \dot{E}_{sw} + \frac{L\tau}{I}$$

$$E''_{sw} = -\frac{L(t''_{sw})^2}{2I} + E_o = E_{sw} - (\dot{E}''_{sw})\tau + \frac{L\tau^2}{2I}$$

or

$$\dot{E}_{sw} = \dot{E}''_{sw} - \frac{L\tau}{I} \tag{2}$$

$$E_{sw} = E''_{sw} + (\dot{E}''_{sw})\tau - \frac{L\tau^2}{2I} \tag{3}$$

Substituting into Eq. (1)

$$E''_{sw} + \left[(\dot{E}''_{sw})\tau - \frac{L\tau^2}{2I}\right] = \frac{I}{2L}\left[\dot{E}''_{sw} - \frac{L\tau}{I}\right]^2$$

rearranging we get

$$E''_{sw} + \frac{L\tau^2}{I} = \frac{I}{2L}\left[\dot{E}''_{sw} - \frac{2L\tau}{I}\right]^2 \tag{4}$$

This is the trajectory of the lower advanced switching line with apex occurring at $E''_{sw} = -L\tau^2/I$ and $\dot{E}''_{sw} = 2L\tau/I$. Similarly the trajectory of the upper advanced switching line is

$$\left[E''_{sw} - \frac{L\tau^2}{I}\right] = -\frac{I}{2L}\left[\dot{E}''_{sw} + 2L\tau/I\right]^2 \tag{5}$$

Its apex occurs at $E''_{sw} = -L\tau^2/I$ and $\dot{E}''_{sw} = -2L\tau/I$. These advanced switching lines are the commanded switching lines required in the presence of a time delay. They are shown in Fig. 2-7.

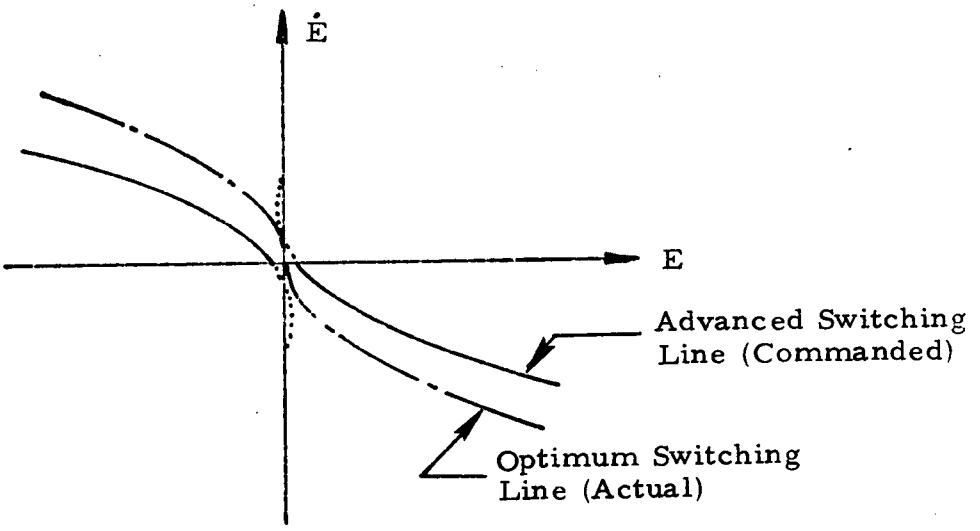

Fig. 2-7 - Phase Plane Representation of Advanced Switching Lines to Compensate for Time Delays

Equations (4) and (5) reduce to the optimum switching line when $\tau = 0$ (no time delay).

$$E''_{sw} = \frac{I}{2L}\left[\dot{E}''_{sw}\right]^2 \qquad \text{lower switching line}$$

$$E''_{sw} = -\frac{I}{2L}\left[\dot{E}''_{sw}\right]^2 \qquad \text{upper switching line}$$

or

$$E''_{sw} = -\frac{I}{2L}\,\dot{E}''_{sw}\left|\dot{E}''_{sw}\right| \tag{6}$$

Implementation of Eqs. (4) and (5) is considerably different from that of Eq. (6) and would require a major reprogramming effort. However, for most cases, the time delay and L/I are fairly small so that Eqs. (2) and (3) can be approximated by:

$$\dot{E}_{sw} \cong \dot{E}''_{sw}$$

$$E_{sw} \cong E''_{sw} + \dot{E}''_{sw}\tau$$

The approximated switching lines can be written as

$$E''_{sw} + \dot{E}''_{sw}\tau \cong -\frac{I}{2L}\,\dot{E}''_{sw}\left|\dot{E}''_{sw}\right|$$

which has the same form as Eq. (6). The only change made in the raw control law was to replace E by $E + \dot{E}\tau$.

The objective of the zero velocity control law is to eliminate limit cycles and to provide a sufficient buffer for the analog computer noises. The presence of time delay can cause unnecessarily large residue velocities due to excessive firing. These large residue velocities often lead to fast drift and make the system more oscillatory. In order to prevent this

shortcoming, the commanded no-firing regions inside the deadzone and in the first and third quadrants on the E, $\dot{E}$ plane were enlarged (see Fig. 2-8). The enlarged areas correspond to that velocity increment, ΔV, which would result from continuous firing for a time span of sampling period plus time delay. This change in the zero velocity control laws ensures that the velocity of the system in the second and fourth quadrants is always small, thus decreasing drift and making the system less oscillatory. Note that the actual no-fire region remains unchanged.

Translation control for automatic docking is accomplished using the two-burn translation logic developed in Ref. 2. This logic attempts to complete docking in a specified (input) time using a maximum of two burn periods in each axis. A separate deadzone logic holds the docked position once it is reached. This deadzone logic acts independently in each axis and requires that the chaser stay in local vertical attitude hold during automatic docking. This system produces minimum fuel docking translation when coriolis, gravitational and centrifugal terms are neglected in the translation equations.

2.5 MANUAL CONTROL

Chaser control during the manual mode is modeled after the Lunar Module Reaction Control System used in Ref. 1. Translation maneuvers are made by commanding control forces along chaser body axes. The chaser is permitted to coast when translation commands are zero. The attitude control logic which is described below maneuvers by rate commands. System delays are simulated by delaying all commands by 0.14 second before their effect is felt through the thrusters.

The chaser angular rates are compared with pilot commanded rates, P_c, Q_c and R_c, from the attitude hand controller. The resulting error signals, $\dot{E}_i$, are fed back to the control logic. The subscript i will be used throughout this discussion to represent the chaser body (principal) axes, XB, YB and ZB.

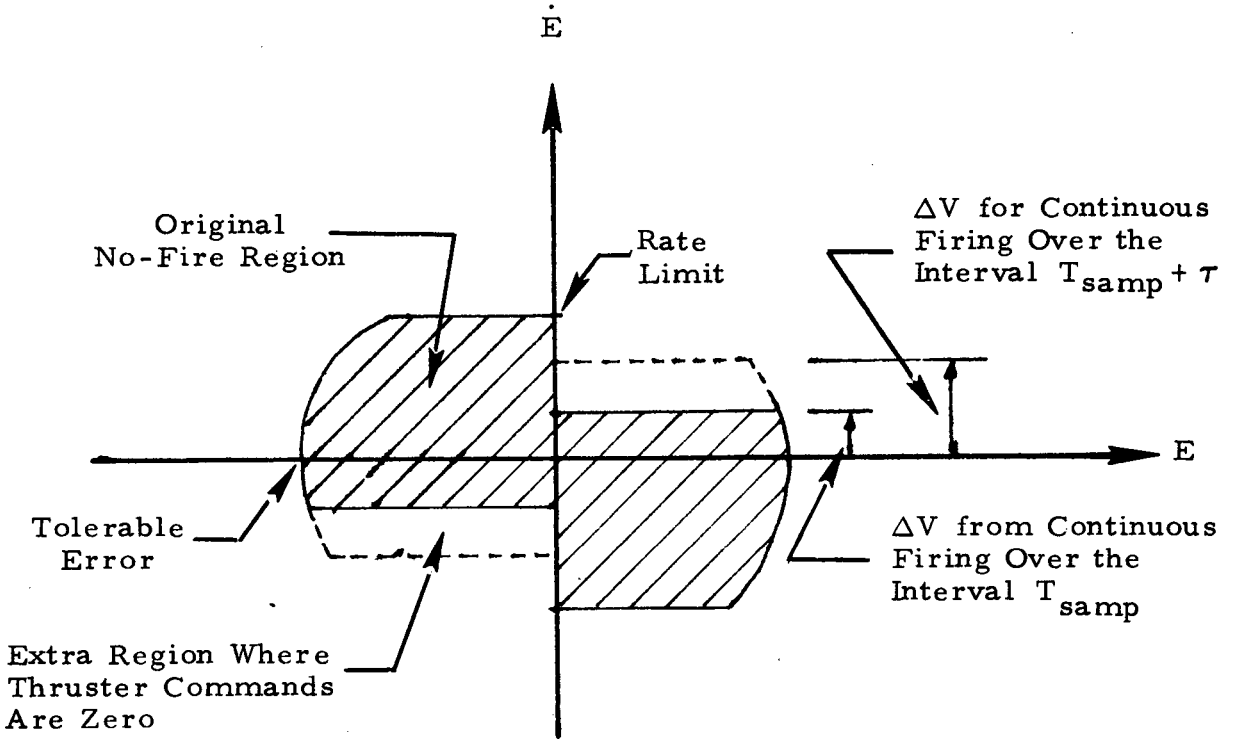

Fig. 2-8 - Enlarged Phase Plane Region for Zero Thruster Commands to Compensate for System Time Delay, τ.

There are two modes of manual attitude control, a maneuvering mode and an attitude hold mode. The maneuvering mode is used whenever there are rate commands from the attitude hand controller i.e., whenever P_c, Q_c, and R_c are not all equal to zero. In this mode only the angular rate errors about the three-body axes, $\dot{E}_i$, are fed back. These three rate errors are tested against a rate error deadband, as shown below.

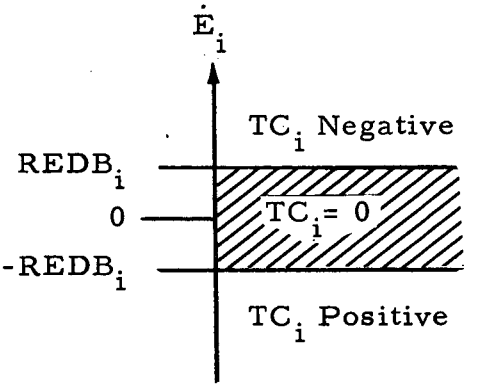

If $\dot{E}_i$ is greater than $REDB_i$ then the manual control logic calls for a negative torque about the i axis. If $\dot{E}_i$ is less than $-REDB_i$ a positive torque is called for. The $REDB_i$ are computed internally as a function of chaser inertia characteristics, control torques, and digital sample time.

$$REDB_i = (5.)(DEL_i)$$

$$DEL_i = (\hat{T}SAMP)(TC_i/I_{ii})$$

Note that vehicle attitude is allowed to drift in this mode.

Whenever there are no rate commands (i.e., $P_c = Q_c = R_c = 0$) the attitude hold control laws are used. In this mode attitude errors about the body axes are fed back along with the angular rate errors. Figure 2-9 illustrates the phase plane for the attitude hold mode. The parameters which define the torquing regions and coast region are computed as shown in the following:

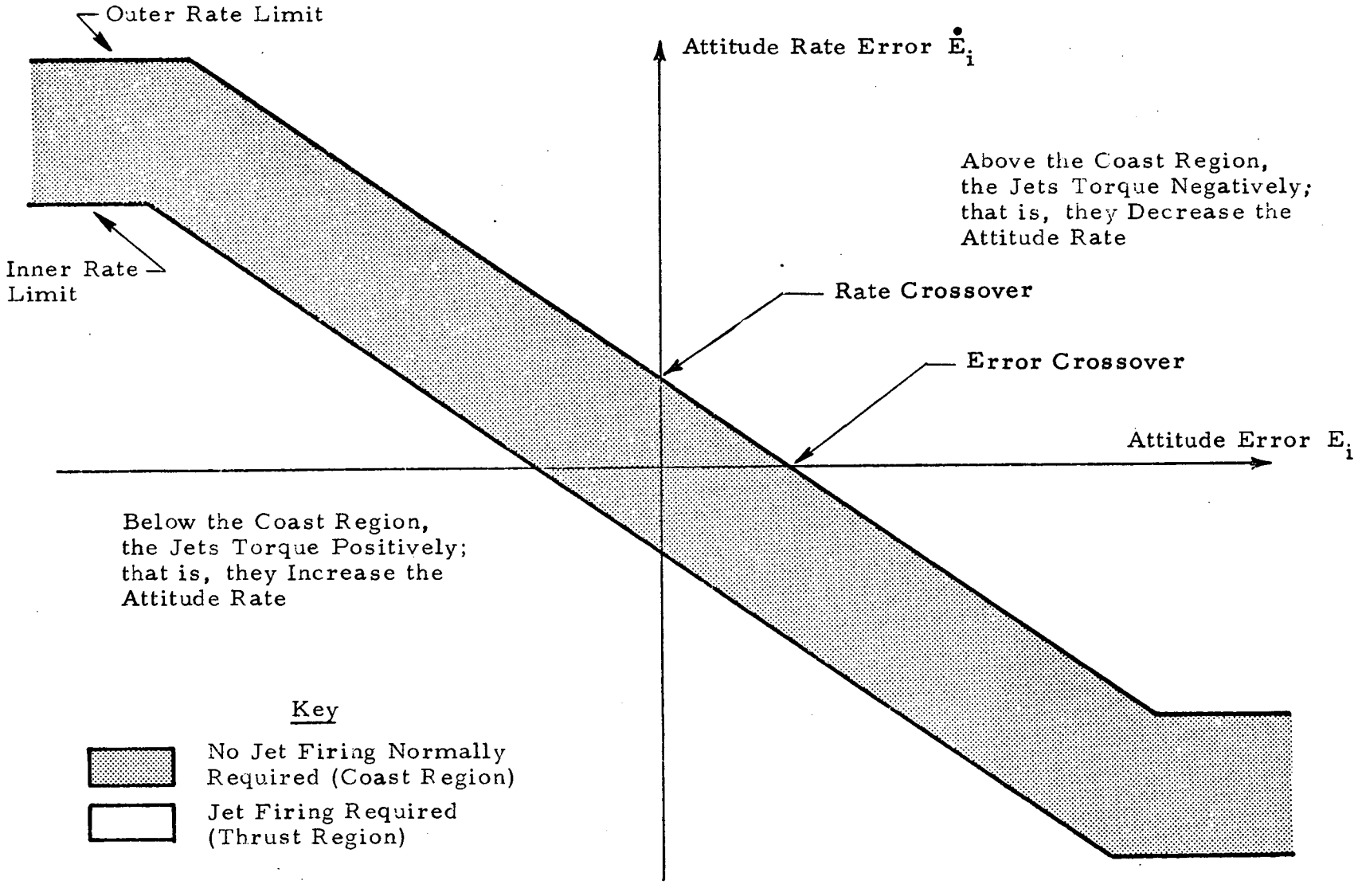

Fig. 2-9 - Phase Plane for Manual Attitude Hold Mode

$$(\text{Outer Rate Limit})_i = (5.)(DEL_i)$$

$$(\text{Inner Rate Limit})_i = (3.)(DEL_i)$$

$$(\text{Rate Crossover})_i = DEL_i$$

$$(\text{Error Crossover})_i = 1.4 \text{ degrees}$$

A new holding attitude is computed every time that the simulation switches to manual attitude hold. When the attitude hold mode is entered, the program starts comparing the three angular rate errors to the outer rate limit in the attitude hold phase plane. As soon as the magnitude of all three $\dot{E}_i$ are less than their corresponding outer rate limit, the holding attitude is set equal to the present inertial attitude. The manual attitude hold mode will then maintain this attitude within the designated deadbands until attitude maneuvers are commanded.

Note that if the attitude rate commands are equal to or less than the outer rate limit, then there will be no attitude coasting when the attitude hand controller is returned to zero. If the rate commands are greater than the outer rate limit however, the astronaut must allow for some attitude coasting after he returns to attitude hold.

2.6 SIMULATION INPUT-OUTPUT

All program input and output has been converted from English to metric units. Inputs are made in three ways — potentiometer settings, card reader inputs, and typewriter inputs. Chaser mass and inertia data, control torque magnitudes, and target orbital rate are input to a digital POT-SET routine. This routine then computes the required potentiometer settings and automatically sets all the required analog potentiometers. Data read in on cards include option flags, control system variables, docking geometry, sensor errors, digital sample time, and initial chaser attitude, velocity, and angular velocity. Chaser initial position, run identification and desired docking time are typed inputs.

The simulation stops automatically when the chase vehicle has successfully docked or crashed. Runs can also be terminated through a manually controlled switch or at a time specified by typed input. Upon run termination the digital computer prints out the case number, the initial conditions, and the reason for termination — successful docking, missed attempt, or run flagged off. Also included in the printout are all the end conditions needed to evaluate the docking run, which are:

- Run time
- Fuel consumed and number of jet firings — this is presented separately for automatic mode, manual mode, attitude control, and translation control
- Chaser position, velocity, orientation, and angular rate
- Lateral offset from docking axis
- Lateral velocity
- Roll misalignment
- Axial misalignment
- Axial angular rate.

Some of these docking parameters are illustrated in Fig. 2-10, and the corresponding Apollo design values are listed.

Two strip chart recorders with eight channels each are used to record time histories of some of the docking variables. Usually position, velocity, angular rates, and jet firings are recorded.

Parameter	Apollo Design Values
Closing Velocity	0.030 to 0.3048 m/sec
Lateral Velocity	0.1524 m/sec
Lateral Offset	0.3048 m
Axial Misalignment	10.0 deg
Axial Angular Rate	±1.0 deg/sec
Roll Misalignment	±10.0 deg

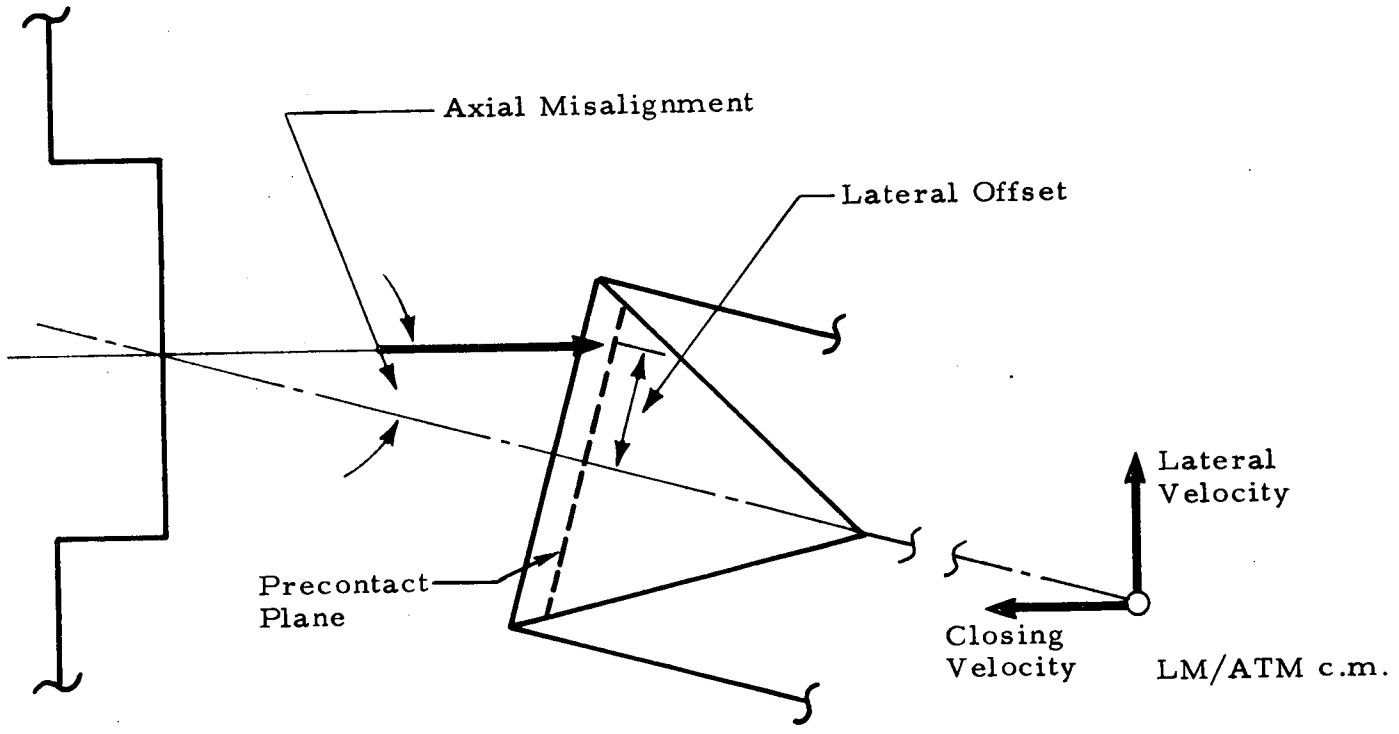

Fig. 2-10 - Docking Parameters Computed After Run Termination

Section 3
SIMULATION RESULTS

Hybrid simulation runs were made using the nominal target and chaser data to verify the program and investigate certain system parameters. Pilot capability to perform during manual control was limited because no hand controllers were available. Manual runs did however verify program subroutines and permitted a qualitative evaluation of the nominal chase vehicle for manual control.

In all manual runs the pilot was located at the chaser center of mass with his viewing direction along the chaser x-axis. Runs showed that manual docking within Apollo design accuracies was possible using a crude switchbox (six three-position switches) for attitude and translation commands. These runs also indicated that the nominal control forces (7340 Newtons) are suitable for accurate manual translation. They produce linear accelerations of 0.06 meters per second^2. The nominal control torques (based on two jets per axis) produce angular accelerations of about 0.18 degree per second^2. These are undesirably low for manual maneuvers. The low accelerations require long attitude maneuvering times which permit error buildup in the non-maneuvering axes. This puts a greater strain on the pilot. Runs with increased control torques (four and six jets per axis) improved manual controllability but resulted in greater fuel consumption.

Automatic docking runs were made to show the effects of initial chaser position, attitude, allowable docking time, and disturbance forces on fuel requirements. In all these runs initial chaser position is expressed in the local vertical coordinates illustrated in Fig. 2-1.

Figure 3-1 shows the fuel required to automatically dock from 305 meters (1000 feet) as a function of docking time. Initial chaser range was equally divided

Initial Position		
x(1)	=	176 m
x(2)	=	176 m
x(3)	=	176 m

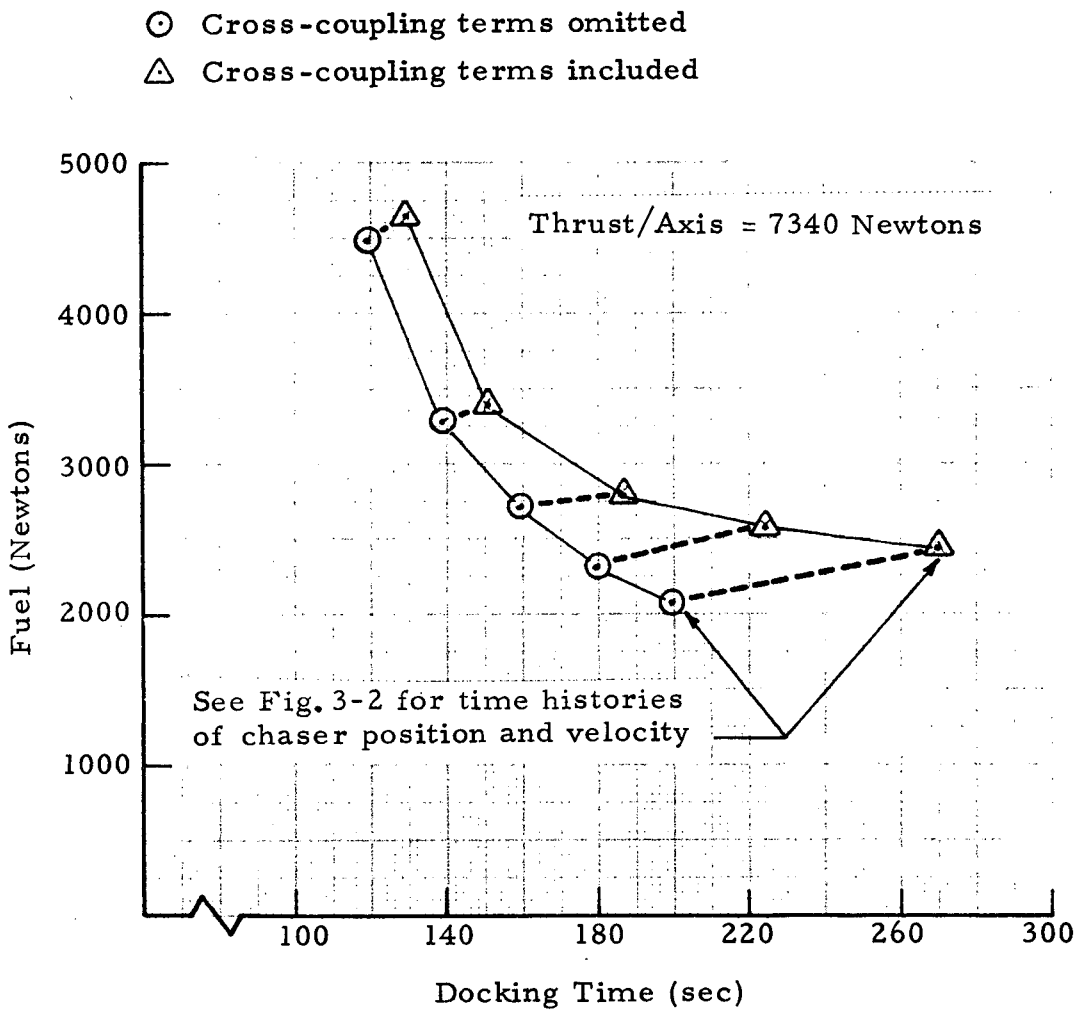

Fig. 3-1- Fuel Required to Automatically Dock from 305 Meters Distance vs Time to Dock

between the three local vertical axes. Chaser attitude errors and velocity were initially zero. Runs were made both neglecting and including the coriolis, centrifugal, and gravitational disturbance forces. These curves show the large fuel savings which result when docking time is increased (i.e., coasting velocity is lowered). The effect of the disturbance terms is primarily to lengthen docking time rather than increase fuel consumption. The fuel used for attitude control increased with docking time but was always less than 7% of the total. Figure 3-2 presents the time histories of chaser position and velocity for the last pair of points in Fig. 3-1. As expected, the disturbance effects are felt in the x(1) and x(2) axes and not in the x(3) axis.

Table 3-1 shows how docking time and fuel requirements are affected by the chaser approach axis. In all six runs the chaser initial range was 300 meters and the desired docking time was 300 seconds.

Table 3-1
TIME AND FUEL TO DOCK VS APPROACH AXIS

Initial Chaser Displacement Axis	Time to Dock (sec)	Fuel to Dock (N)
+x(1)	324	3780
-x(1)	322	3110
+x(2)	298	3130
-x(2)	296	3340
+x(3)	295	1670
-x(3)	296	1430

Figure 3-3 shows how docking fuel requirements increase with range when docking time is kept constant. This figure also shows the maximum coasting velocity for each run.

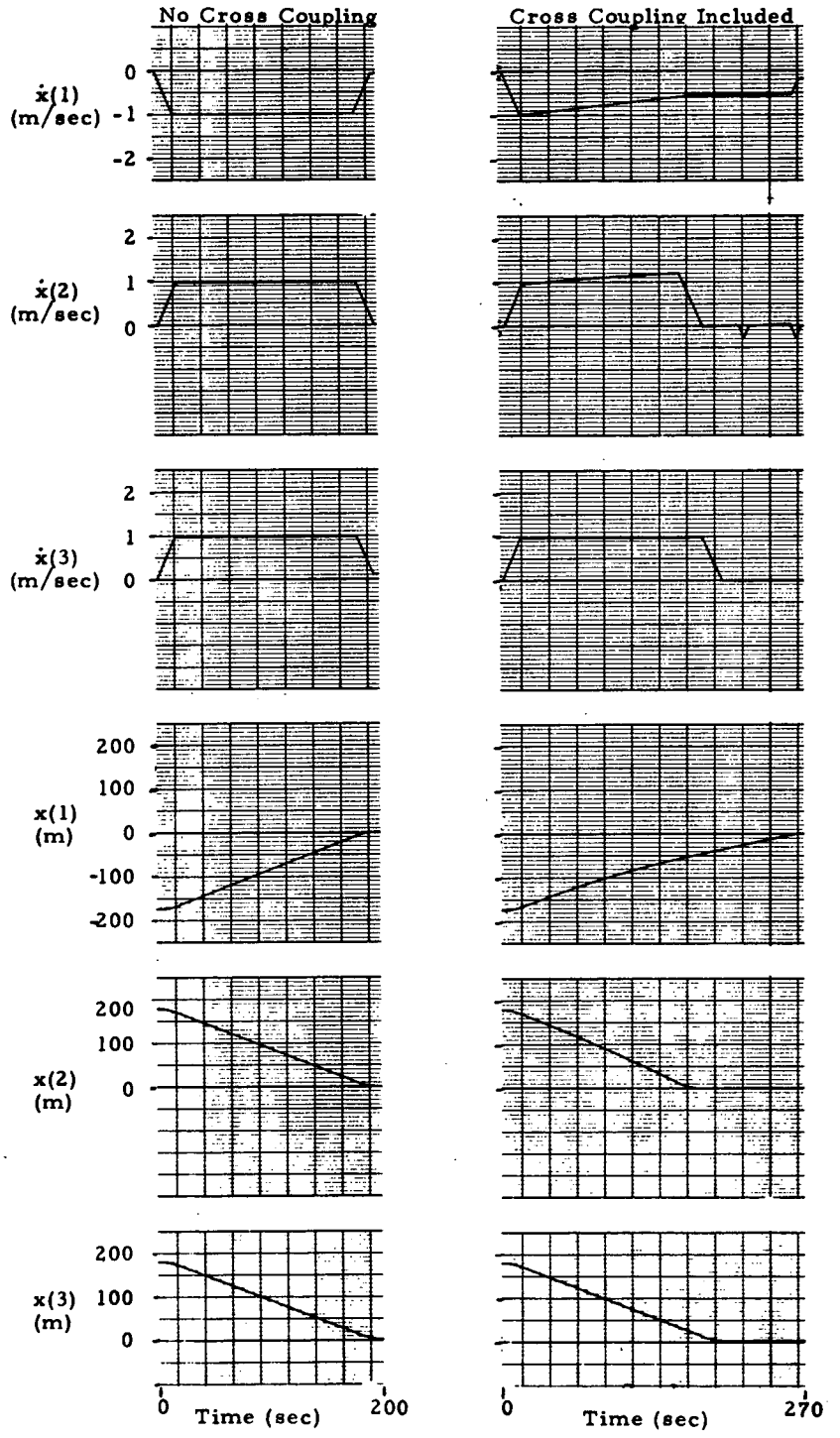

Fig. 3-2 - Time Histories of Chaser Position and Velocity for Runs Shown in Fig. 3-1

Although the results shown above include the fuel required to maintain attitude hold, the runs were all initialized with zero attitude errors and rate errors. Figures 3-4 and 3-5 show the fuel required to eliminate attitude errors and attitude rate errors, respectively.

Simulation runs were made using the switching option (real time switching between automatic and manual control). One sequence which showed promise was to maneuver automatically to a rendezvous point near the docked position and then switch to manual control for final alignment and translation. This method gives low fuel consumption and good accuracy.

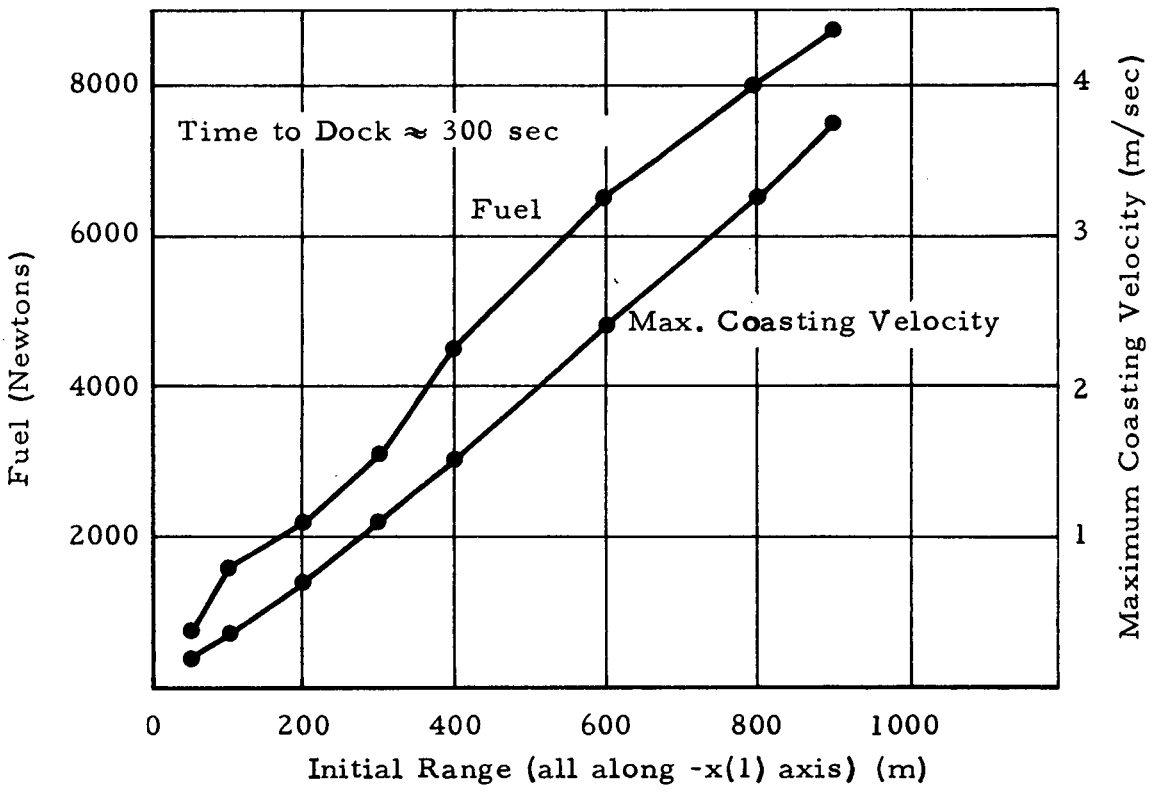

Fig. 3-3 - Fuel Required to Dock and Maximum Coasting Velocity vs Initial Range Along -x(1)

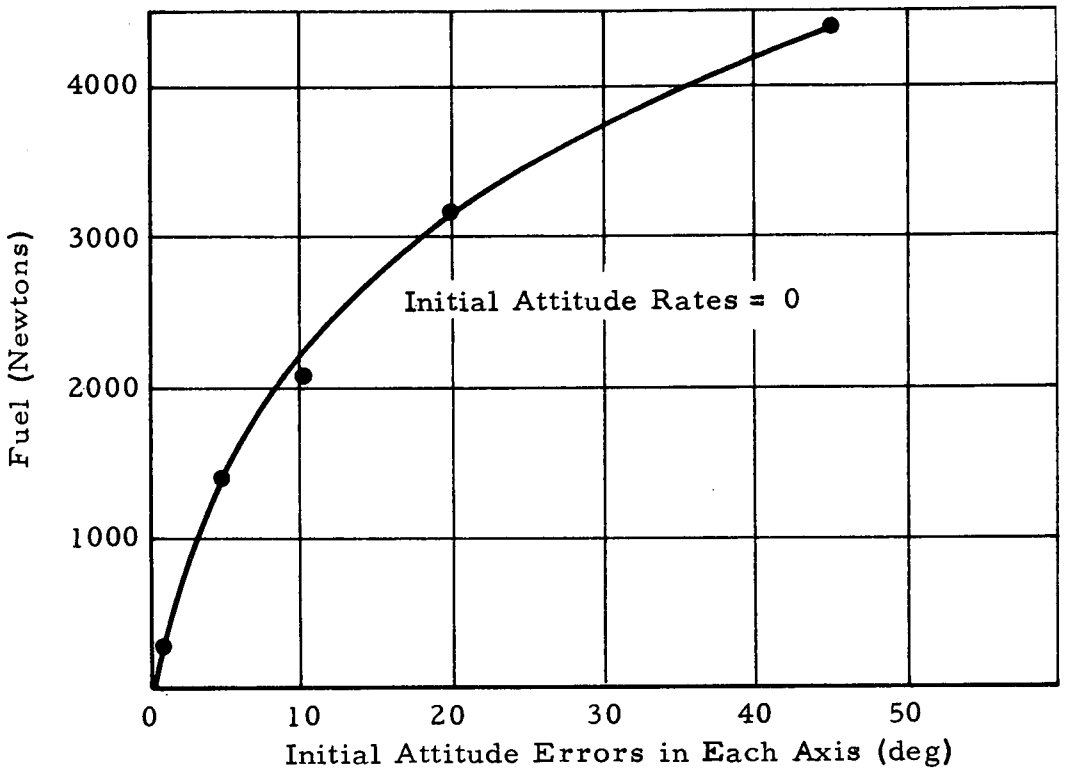

Fig. 3-4 - Fuel Required to Eliminate Initial Attitude Errors

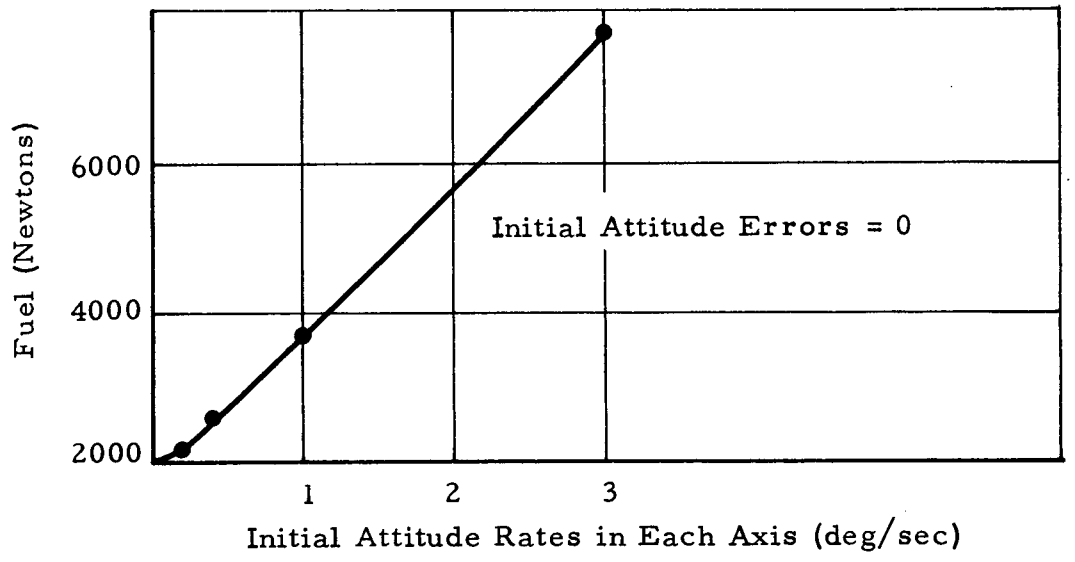

Fig. 3-5 - Fuel Required to Eliminate Initial Attitude Errors

Section 4
CONCLUSIONS AND RECOMMENDATIONS

A versatile hybrid simulation of orbital maneuvers was developed during this study. The program simulates the six-degree-of-freedom motion of a chase vehicle as it maneuvers relative to an orbiting target. A cylindrical representation of the target is displayed on a CRT display scope so that the maneuvers can be visually monitored by a pilot located in the active vehicle. Both automatic and manual control can be simulated. A third option includes real time switching between automatic and manual control at the pilot's discretion. System time delays (presently 0.14 second) are included to represent delays between commands and thruster firings. Another option permits simulation of sensor errors so that their effect on accuracy and fuel consumption can be assessed. General program application has been maintained where possible through modularization and the retention of system parameters as program inputs. Computer runs involving pilot interaction must be made in real time; however those using only automatic control can be made at accelerated run speeds to achieve a savings in computer time.

Computer runs using nominal chaser and target data verified the operational status of the simulation. Both manually and automatically controlled docking runs achieved accuracies within Apollo design limits. Manual attitude controllability was improved at the expense of fuel consumption by increasing the control torques. Automatic docking generally required much less fuel. A two-step docking sequence which yielded low fuel consumption and high accuracy was as follows:

1. Maneuver automatically to a rendezvous point near the docked position.
2. Switch to manual control for final alignment and translation.

Automatic runs showed the fuel advantage of making maneuvers at low coasting velocities. The fuel required to eliminate attitude and attitude rate errors of the nominal chase vehicle was also determined.

Three tasks recommended for continued analysis are described below:

1. Make docking simulation runs to compare the relative merits of purely automatic control, purely manual control, and a combination of both. Also define desirable switching points between automatic and manual control. These runs will require the use of hand controllers for manual translation and attitude commands to add realism to the manual mode. These controllers need supply only on-off capability in the six degrees of freedom. Improvements in the manual mode including minimum impulse bit capability and greater control logic sophistication are needed to reduce fuel requirements.

2. Add the capability to simulate remote docking so that free-flying unmanned Research and Applications Modules (RAM's) can be simulated docking to the space station. This would draw heavily from the remote docking work already completed during Appendix B of the present contract.

3. Modify the program to allow simulation of satellite inspection and retrieval maneuvers. Include the effects from discrete and continuous mass shifts.

Section 5

REFERENCES

1. Heeschen, G. M., "Dynamic Docking Study — Final Report — Appendix B," LMSC-HREC D149063, Lockheed Missiles & Space Company, Huntsville, Ala., July 1969.

2. Heeschen, G. M., and G. R. Hewitt, "Space Shuttle Docking Study — Final Report — Appendix D," LMSC-HREC D162488, Lockheed Missiles & Space Company, Huntsville, Ala., August 1970.

3. Chang, C. J., and G. M. Heeschen, "Dynamic Docking Study Hybrid Simulation — Final Report — Appendix E," LMSC-HREC D162918, Lockheed Missiles & Space Company, Huntsville, Ala., March 1971.

Appendix A

HYBRID SIMULATION DIGITAL FLOW CHARTS AND SUBROUTINE DESCRIPTIONS

Appendix A

A.1 GENERAL

This appendix describes the digital subroutines used in the hybrid simulation. Section A.2 presents a glossary of terms used in this description. Variable dimensions are shown in parentheses if they are greater than one. The glossary includes numerical values for those variables which are set in data statements.

Sections A.3 through A.7 describe five of the major digital subroutines including subroutine flow charts. In these flow charts I is a free index and takes on values of 1, 2 and 3 respectively unless otherwise stated. An asterisk (*) preceding a statement identifies it as a hybrid operation. Statements enclosed in quotation marks are messages printed out on the typewriter.

Simulation timing and interrupts are described in Section A.8

A.2 GLOSSARY OF TERMS

Term	Description
ABRNA, ABRNT	jet firing time during automatic portions of the docking sequence for attitude control and translation, respectively.
ADC(16)	hybrid variables which are sent from the analog side to the digital side.
ADSCAL(16)	scaling factors relating analog and digital values of ADC(16) (see Table A-1).
ALFAF	scale factor to adjust the display field of view.
ALT	orbital altitude of target (5.0003×10^5 m).
ANS	typed input (yes or no) which determines if the simulation run will be automatically stopped at some input time (TFLAG).
ASTART	number of jet starts during automatic portions of docking sequence.
AXMIS	axial misalignment of the chaser at the end of the docking run.
BIXYZ(3)	chaser principal moments of inertia (see Table A-2).
BRNA, BRNT	jet firing time for attitude control and translation, respectively.
BV(3, 3)	transformation matrix from chaser to local vertical coordinates.
D(3), DD(3)	chaser position and velocity relative to the rendezvous point expressed in jet axes.
DAC(16)	hybrid variables which are sent from the digital side to the analog side.
DASCAL(16)	scaling factors used in subroutine ALOGIC to relate analog and digital values of DAC(16) (see Table A-1).

Term	Description
DEL(3)	maximum change in chaser body rates during one digital sample time.
DISTLV(3)	chaser position relative to the rendezvous point in local vertical coordinates.
DISTB(3)	chaser position relative to the rendezvous point in body coordinates.
DSSCAL(16)	scaling factors used in subroutine HLOOP to relate analog and digital values of DAC(16) (see Table A-1).
E(3)	chaser attitude errors.
EDOT(3)	chaser attitude rate errors.
EPSI(3)	Euler angles used to input the initial chaser attitude.
EYE	inclination of target orbit (0 deg).
E1DD	attitude error deadband for automatic attitude control.
E2DD	used to define automatic attitude control deadzone.
E2S	rate limit during automatic attitude control.
F(3)	control forces acting on chase vehicle in local vertical coordinates.
FB(3)	control forces acting on chase vehicle in body coordinates.
FBRNA, FBRNT	jet firing time for attitude control and translation, respectively.
FCXP, FCYP, FSXP, FSYP	factors used to generate the circle projections in the docking target display.
FFA	fraction of TSAMP used for minimum impulse bit jet firings.
FLAG1	a manually controlled flag which terminates the run.
FSTART	total number of jet starts (floating point).

Term	Description
FUEL	total fuel consumed during docking sequence.
FX, FY, FZ	translation commands (+1, -1, 0) in chaser body coordinates. These come from the pilot through the hand controller during manual control.
FXYZ(3)	control force per jet along the chaser body axes.
GGCON(3)	constants used to calculate gravity gradient torques on the chaser.
GN(9)	current set of gaussian variables from table look-up.
GSCAL	chaser position scaling factor to permit higher accuracy at close range.
HBRNA, HBRNT	jet firing times during manual portions of the docking sequence for attitude control and translation, respectively.
HSTART	number of jet starts during manual portions of docking sequence.
ICHAN	channel number (ADC or DAC) which caused flag IERR to be set.
IDENT	typed input for run identification.
IDOCK	program control flag { +1 successful dock. 0 not yet docked. -1 missed attempt.
IERR	a flag to indicate an overload in the ADC or DAC channels.
IFL(6)	input program control flags (described in Table A-3).
IFL6I	input value of IFL(6) { 0 = automatic control. 1 = manual control.
IGN	counter (1-1000) for gaussian variables.
IMAN	flag which detects a change in control mode (automatic or manual).

Term	Description
INITAL	program control flag (negative the first time through subroutine HLOOP).
IPGMGR, ISTEER	program control flags.
JET(I)	state of attitude control jets commanded by automatic control laws (+1, 0, -1).
/JETPRV	non-FORTRAN variable used to switch between automatic and manual control and controlled by the pilot.
JJT(3)	state of attitude control jets sent to the analog (+1, 0, -1).
MANCL	flag which is non-zero during manual attitude maneuvers.
N	counter for digital clock.
ONE(3)	upper switching line for manual attitude hold control laws.
OPER	orbital period of target in seconds.
ORL(3)	attitude rate limit under manual control.
P(3)	initial chaser body rates (RATEB(3)).
PI	3.14159.
PMI	range from chaser to target docking collar at which run terminates.
PM2	location of rendezvous point along target docking axis measured from the target center of mass.
PQRCMD	a flag which is greater than zero whenever attitude changes are commanded under manual control.
QBR(4)	quaternions relating chaser attitude to chaser reference attitude and used to compute attitude errors during automatic control.
QIB(4)	quaternions relating inertial coordinates to chaser body coordinates.

Term	Description
QIBD(4)	desired values of QIB(4) for periods of attitude hold under manual control.
QIV(4)	quaternions relating inertial coordinates to local vertical coordinates.
QVB(4)	quaternions relating local vertical coordinates to chaser body coordinates.
QVR(4)	constant quaternions which describe the target attitude relative to inertial or local vertical coordinates.
RADIUS	radius of the end circles for the cylindrical representation of the docking target.
RANG, RANGR	chaser to target range and range rate, respectively.
RATEB(3)	angular rates about chaser body axes.
RE	radius of the earth-spherical equivalent (6.36743×10^6 m).
REF(3)	Euler angles relating inertial or local vertical coordinates to target coordinates.
RERR, RRERR	per unit error in measuring chaser to target range and range rate, respectively.
RF(3, 3)	transformation matrix from inertial or local vertical coordinates to target coordinates.
RHOZM, RHOZP	distances from target center of mass to the rear and front faces of the cylindrical representation, respectively.
RNATT	number of jets per axis used to produce chaser control torques.
RNTRAN	number of jets per axis used to produce chaser control forces.
ROLMIS	chaser roll misalignment at the end of the docking run.
RPD	radians per degree (0.017453292).

Term	Description
RSLOPE	display parameter to size the rear face of the target.
S(3)	slope of the manual attitude control law switching curve.
SIGMA(10)	standard deviations to describe sensor errors.
SIGR, SIGRR	standard deviation for range and range rate measurements, respectively.
SPECI	fuel specific impulse (352 sec).
STARTS	total number of jet starts (integer).
TAB(1000)	input table of gaussian numbers.
TAUTO	time spent under automatic control.
TB2T(3, 3)	transformation matrix from chaser to target coordinates.
TCMAG(3)	magnitude of chaser control torques.
TDELAY	system time delay between control commands and firing of the jets.
TFLAG	time at which the simulation run is to be flagged off.
TG(3)	gravity gradient torques about chaser body axes.
THRUST	thrust per control jet (7340 N).
TIME	time elapsed since start of docking run.
TIMEF	desired time to complete docking; must be $\geq$ TMIN.
TIMEFI	input TIMEF.
TMAN	time spent under manual control.
TMARG	safety margin on TMIN.
TMIN	minimum time required to achieve automatic docking.
TORQN(3)	control torque per jet about chaser body axes (see Table A-2).

Term	Description
TSAMP	digital sample time.
TWO(3)	lower switching line for manual attitude hold control laws.
U(3)	state of the translation control jets (+1, 0, -1).
UDOT	target orbital rate.
VB(3, 3)	transformation matrix from local vertical to chaser coordinates.
VMU	gravitational constant times the mass of the earth (3.991×10^{14} N-m^2/kg).
V1M(3), V2M(3)	translation dead-zone position and velocity boundary, respectively, in each local vertical axis.
V20(3)	initial chaser velocity (XDOT(3)) in local vertical coordinates.
X(3), XDOT(3)	chaser position and velocity, respectively, in local vertical coordinates.
XB(3), XBD(3)	chaser position and velocity with respect to the target center of mass in chaser body coordinates.
XBM(3), XBDM(3)	measured values of XB(3) and XBD(3) with sensor errors included.
XCLZP, YCLZP	display parameters which locate the front face of the docking target.
XDOCA, XDDOCA	chaser position and velocity relative to the target coordinates.
XIRL(3)	inner rate limit for manual attitude control laws.
XLATOF	chaser lateral offset from the docking axis.
XLATVE	chaser velocity perpendicular to the docking axis.
XM	chaser mass (1.26443×10^5kg).

Term	Description
XQIB	square root of the sum of the squares of QIB(4); should be equal to 1 for orthogonality.
XSCR(3)	position of pilot observation point in chaser body coordinates.
XSLOPE, YSLOPE	display parameters which determine the target orientation.
XSPOT, YSPOT	display parameters to locate the bright spot on the target front face.
Z	target orbital position at the end of the docking run.

A.3 SUBROUTINE MAIN

MAIN is primarily a bookkeeping routine. It performs all normal (non-error) input and output operations and does much of the initialization required before each run. Upon run termination it processes the output data, prints it on the in-line printer, and then returns program control to the typewriter. Figure A-1 shows the flow of subroutine MAIN. Other subroutines which are called from MAIN are briefly described below in the order that they are called.

COEF	– Computes constant parameters for the automatic attitude control logic.
BEGIN	– Performs program initialization including the computation of initial quaternions and transformation matrices.
AUTOIN(D, DD)	– Initializes automatic translation control logic (see Section A.4).
ALOGIC	– Sends chaser initial conditions (position, velocity, attitude, and attitude rate) to the analog computer.
HLOOP	– Performs all digital operations required during the simulation. (see Section A.5)
MAYMUL (O, A, B, C, N)	– A matrix multiplication routine which computes the matrix [C] as follows: $[C] = [A][B]$ N is the number of columns in [C]

A.4 SUBROUTINE AUTOIN

AUTOIN is entered everytime that the simulation is switched into the automatic control mode. This routine initializes the automatic translation control laws so that docking is achieved at the time originally commanded (TIMEFI) if possible. If the time available is too small it attempts to dock in minimum time. A flow chart of AUTOIN is shown in Fig. A-2.

A.5 SUBROUTINE HLOOP

This is the main hybrid subroutine. It completes the initialization of each run and then controls all hybrid and digital operations required during the simulation. Figure A-3 is a flow chart of subroutine HLOOP. Other digital subroutines which are called from HLOOP are briefly described below in the order that they are called.

HLQUAT	computes range, range rate, rendezvous point location, and all transformation matrices required during the run.
DISPLV	computes the 11 variables required to generate the CRT display. The display equations are documented in Ref. 3. This routine also checks to see if docking is completed or if a missed attempt has occurred.
AUTO	computes jet commands under automatic control (see Section A.6).
MANUAL	computes jet commands under manual control (see Section A.7).
TESTSL (1, PQRCMD)	tests for manual attitude rate commands from the pilot.
TMFCMD	tests for the control mode (manual or automatic) and then tests for manual translation commands from the pilot.
AUTOIN(D, DD)	initializes automatic translation control logic (see Section A.4)
OUT(1625)	prints out the contents of the flag register.

The timing of data transfer between the digital and analog computers is controlled by interrupts in such a way as to produce a system time delay of 0.14 second. The timing and interrupts are described in Section A.8.

A.6 SUBROUTINE AUTO

This subroutine computes the commanded control forces and torques during periods of automatic control. Figure A-4 is a flow chart of subroutine AUTO. The three subroutines called from AUTO are briefly described below.

ROTLAW(I)	computes the desired state of the torque jets to maintain attitude hold. This subroutine was developed in a previous study and is fully described in Ref. 3.
TJETS(A, B)	computes the desired state of the translation jets to achieve docking using the baseline two-burn logic. This subroutine was developed in a previous study and is fully documented in Ref. 2.
MAYMUL (O, A, B, C, N)	matrix multiplication routine described in Section A.3.

The torque commands (JJT(I)) and force commands (F(I)) are delayed by 0.14 second before being sent to the analog computer.

A.7 SUBROUTINE MANUAL

MANUAL computes the torque commands (JJT(I)) during periods of manual control according to the switching logic described in Section 2.5. A flow chart of this subroutine is presented in Fig. A-5.

A. 8 SIMULATION TIMING AND INTERRUPTS

During the simulation program variables are transferred between the digital and analog computers in the following ways.

1. Sixteen digital-to-analog (DAC) conversion channels.
2. Sixteen analog-to-digital (ADC) conversion channels.
3. Sixteen logical data bits (+ or 0) from digital to analog through the data word.
4. Sixteen logical data bits (+ or 0) from analog to digital through the data word.
5. Eight hard-wired sense lines.

This data transfer is pictured in Fig. A-6. Three digital subroutines involved in the transfer of data (TMFCMD, JETFIR, and TESTSL) are also pictured and described below.

TMFCMD	interrogates the data word from the analog for control mode (manual or automatic) and manual translation commands.
JETFIR	sends the attitude jet firing commands to the analog via the data word; also processes all jet firings to calculate the number of jet starts, translation burn periods, and rotational burn periods.
TESTSL	interrogates the sense lines for manual attitude rate commands.

Simulation timing is controlled from the digital by the two interrupts shown in Fig. A-7. The timing sequence for the first 0.54 second of the simulation is shown in Fig. A-8. Clock interrupts F_i and T_i represent interrupts "FROM" and "TO," respectively.

During F_1 (at time = 0) the control status (manual or automatic) and the manual force commands (MFCMD) are sampled in subroutine TMFCMD. The initial values from the analog are stored in the ADCs at this time also. The ADCs are inhibited from storing new analog values until the ADC-EBL line (on the analog) goes high. This occurs every 100 milliseconds (after t=0). The ADC-EBL pulses are obtained by counting 100 pulses from the analog 1 kc clock source. The width of the ADC-EBL pulses is determined by the time required to store the analog values in parallel and sequentially convert to digital information in the main stream of subroutine HLOOP. The clock interrupts initiate sampling of the analog information (via the ADCs and data word) and sending information (via DACs and data word) to the analog.

In order to sample MFCMD at the same time the analog values are stored in the ADCs (interface), an initial time of 100 milliseconds is counted

first. When interrupt F_2 occurs the control status (CS) and MFCMD are sampled in subroutine TMFCMD. Then 40 milliseconds is loaded into the digital timer. After the 40 milliseconds interval, interrupt T_1 occurs and the computed information from F_1 is sent to the analog in subroutine JETFIR. The effect of this timing is to produce a delay of 140 milliseconds between the commands and their effect on the vehicle dynamics. The timer is then loaded with 60 milliseconds so that the next interrupt (F_3) will occur at the same time that the ADC-EBL line goes high to sample new analog information. The interrupts occur every 40, then 60 milliseconds until the simulation is completed or aborted. This coincides with the 100 millisecond ADC-EBL pulses.

There is no conflict in timing if the digital computation can be completed in less than 100 milliseconds because the digital cannot execute the instruction to store the analog values until the ADC-EBL line goes high. Therefore, the digital will wait until it can execute the store instruction and then proceed with the computation. The time to complete the computation is typically less than 40 milliseconds. A third interrupt which operates in HLOOP is shown below. This interrupt is executed anytime a timing error occurs.

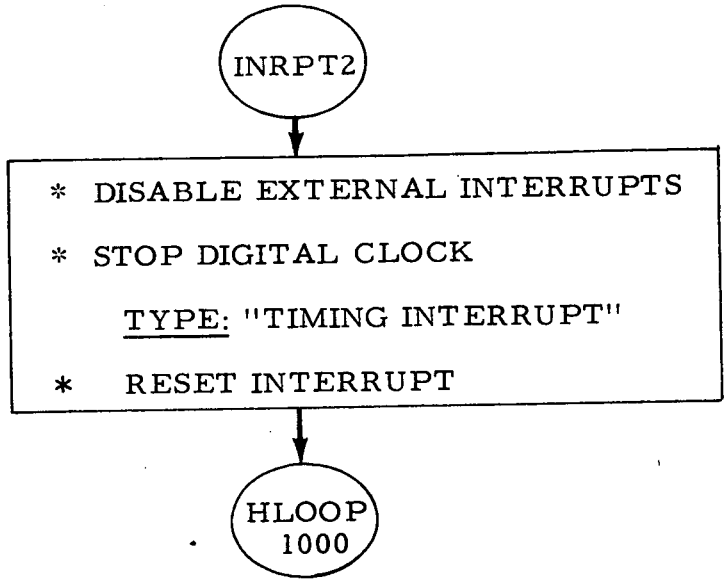

TIMING ERROR
INTERRUPT

Table A-1

NOMINAL VALUES FOR ANALOG-TO-DIGITAL AND DIGITAL-TO-ANALOG SCALING

I	ADSCAL(I)	DASCAL(I)	DSSCAL(I)
1	0.1	0.00001	1.0
2	0.1	0.000005	1.0
3	0.1	0.000005	1.0
4	50.0	0.025	-1.0
5	50.0	0.025	0.025
6	50.0	0.025	0.025
7	-5.0	0.00005	0.00005
8	-5.0	0.00005	0.00005
9	-5.0	0.00005	0.00005
10	2.0	0.0	1.0
11	2.0	0.0	1.0
12	2.0	0.0	-1.0
13	2.0	0.0	1.0
14	0.1	0.0	1.0
15	0.1	0.0	-1.0
16	0.1	0.0	-1.0

Table A-2

NOMINAL VALUES FOR CHASER PRINCIPAL MOMENTS OF INERTIA AND CONTROL TORQUES PER THRUSTER

I	BIXYZ(I) ($kg\text{-}m^2$)	TORQN(I) (N-m)
1	4.203×10^6	1.3558×10^4
2	2.052×10^7	2.8811×10^4
3	2.319×10^7	2.5421×10^4

Table A-3

PROGRAM OPTIONS BY INPUT FLAGS - IFL(I)

FLAG	Option Description	Input Value
IFL(1)	Target in local vertical hold	1
	Target in inertial hold	2
IFL(2)	Perfect sensors	0
	Effect of sensor inaccuracies included	1
IFL(3)	Control torques ≡ 0	0
	Baseline automatic attitude control	1
IFL(4)	Control forces ≡ 0	1
	Translation jets aligned with local vertical axes	2
	Translation jets aligned with body axes	3
	Same as above and including sensor errors	4
IFL(5)	Not currently used	
IFL(6)	Automatic control	0
	Manual control	1

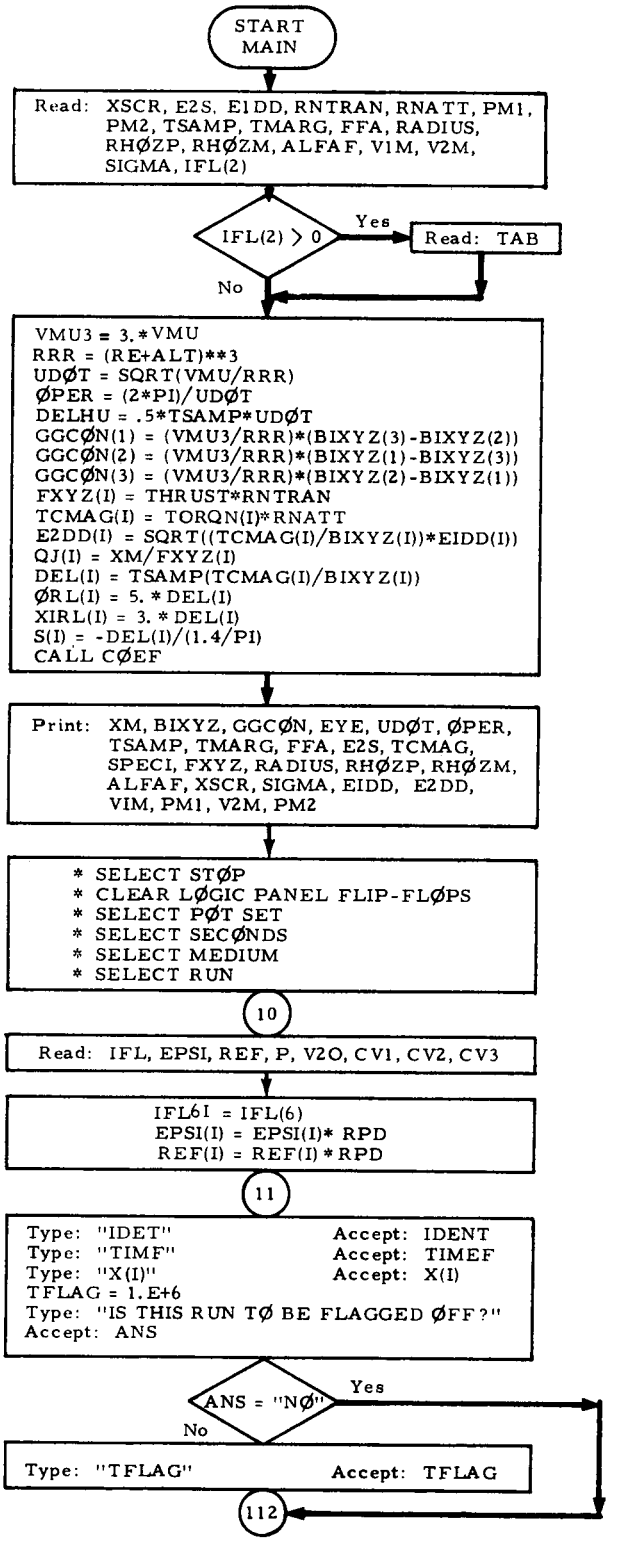

Fig. A-1 - Flow Chart of Subroutine MAIN

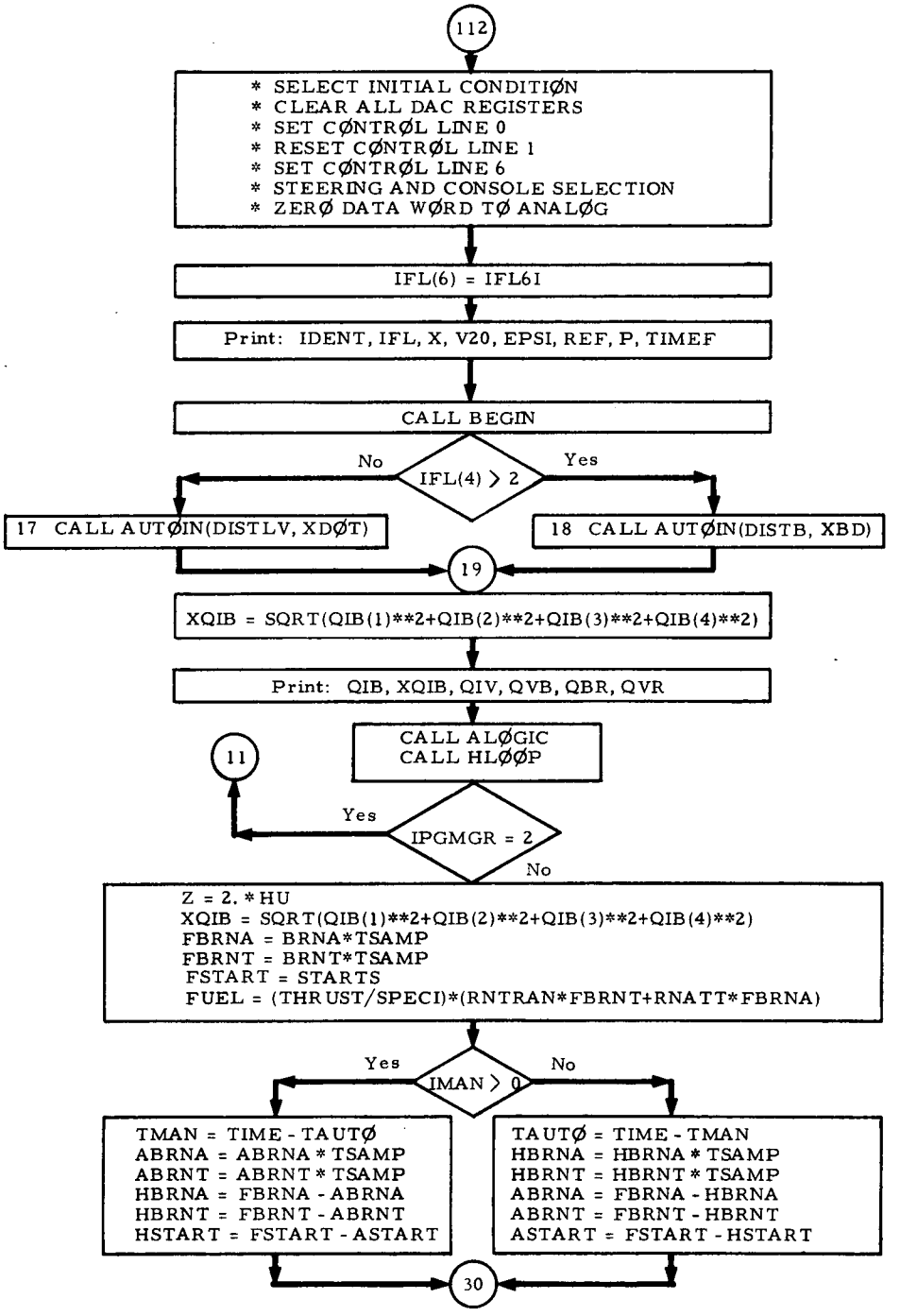

Fig. A-1 - (Continued)

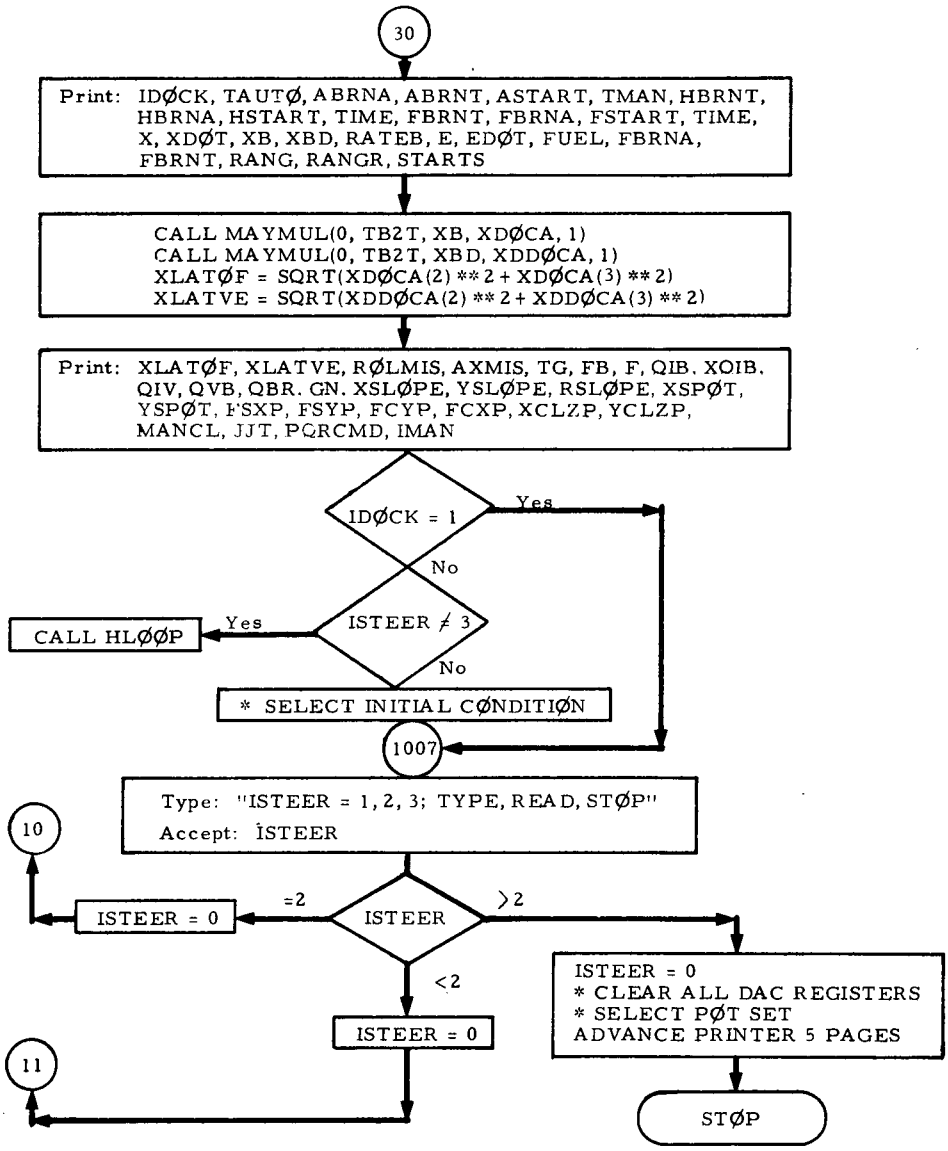

Fig. A-1 - (Concluded)

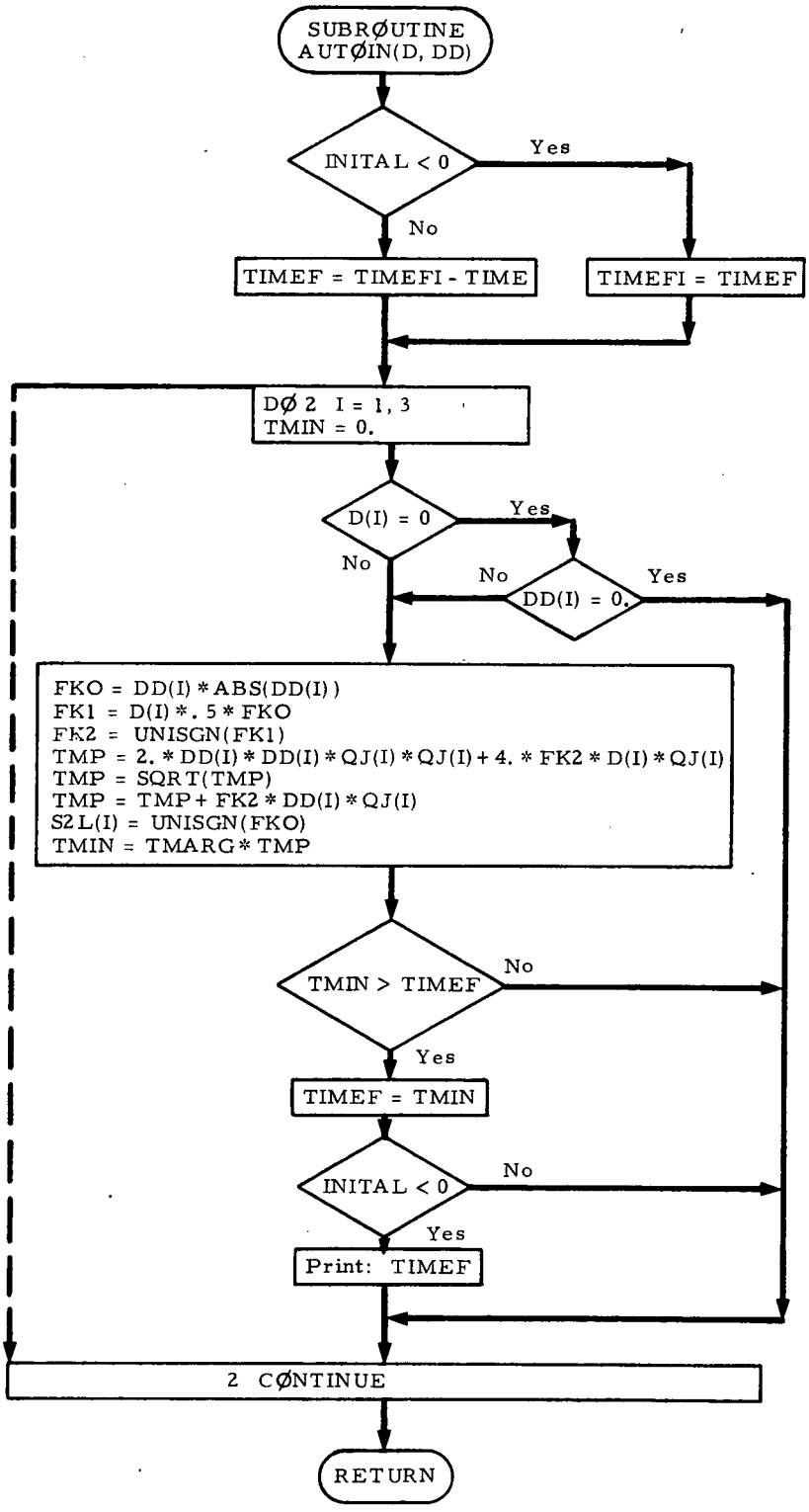

Fig. A-2 - Flow Chart of Subroutine AUTOIN (D, DD)

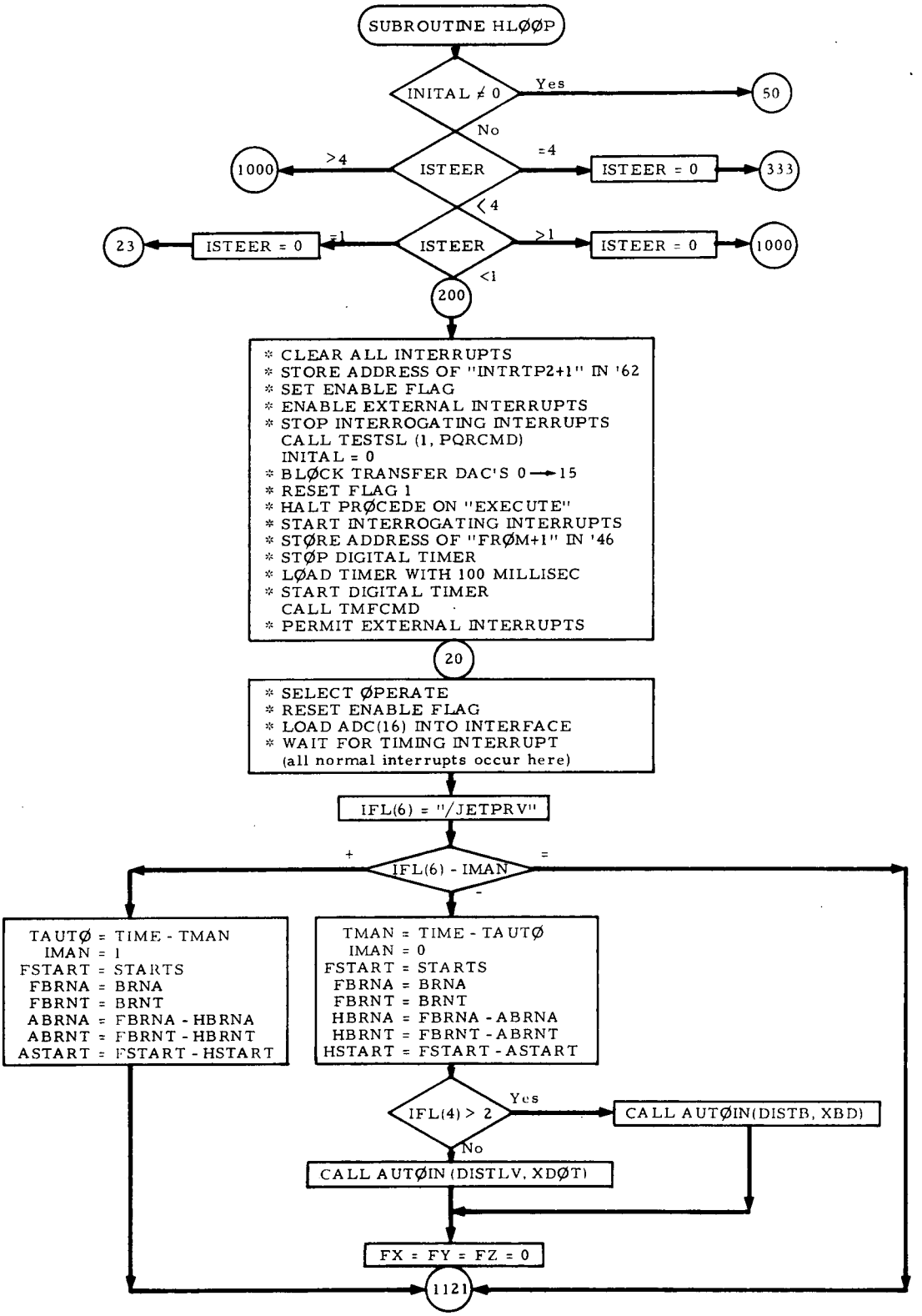

Fig. A-3 - Flow Chart of Subroutine HLOOP

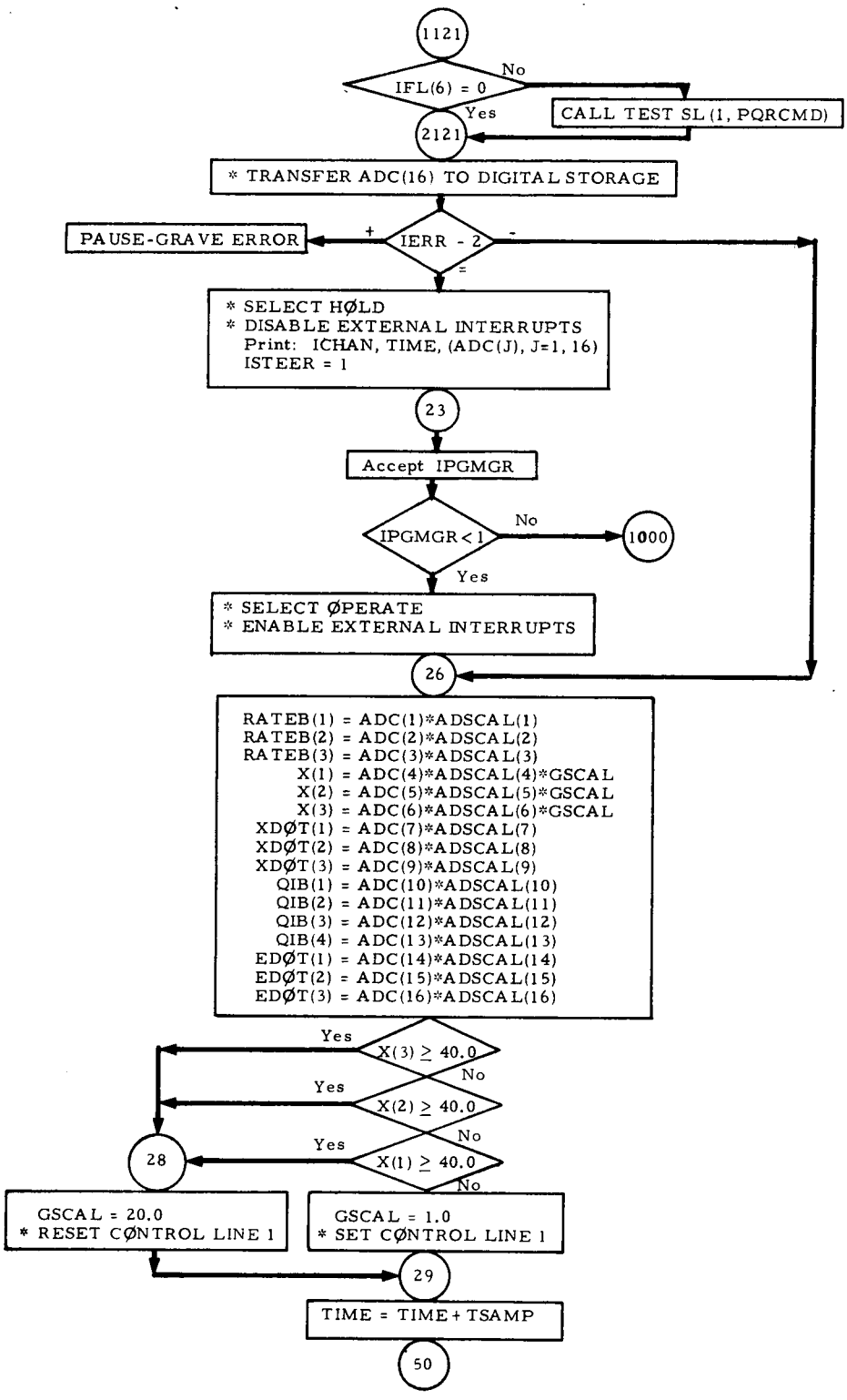

Fig. A-3 - (Continued)

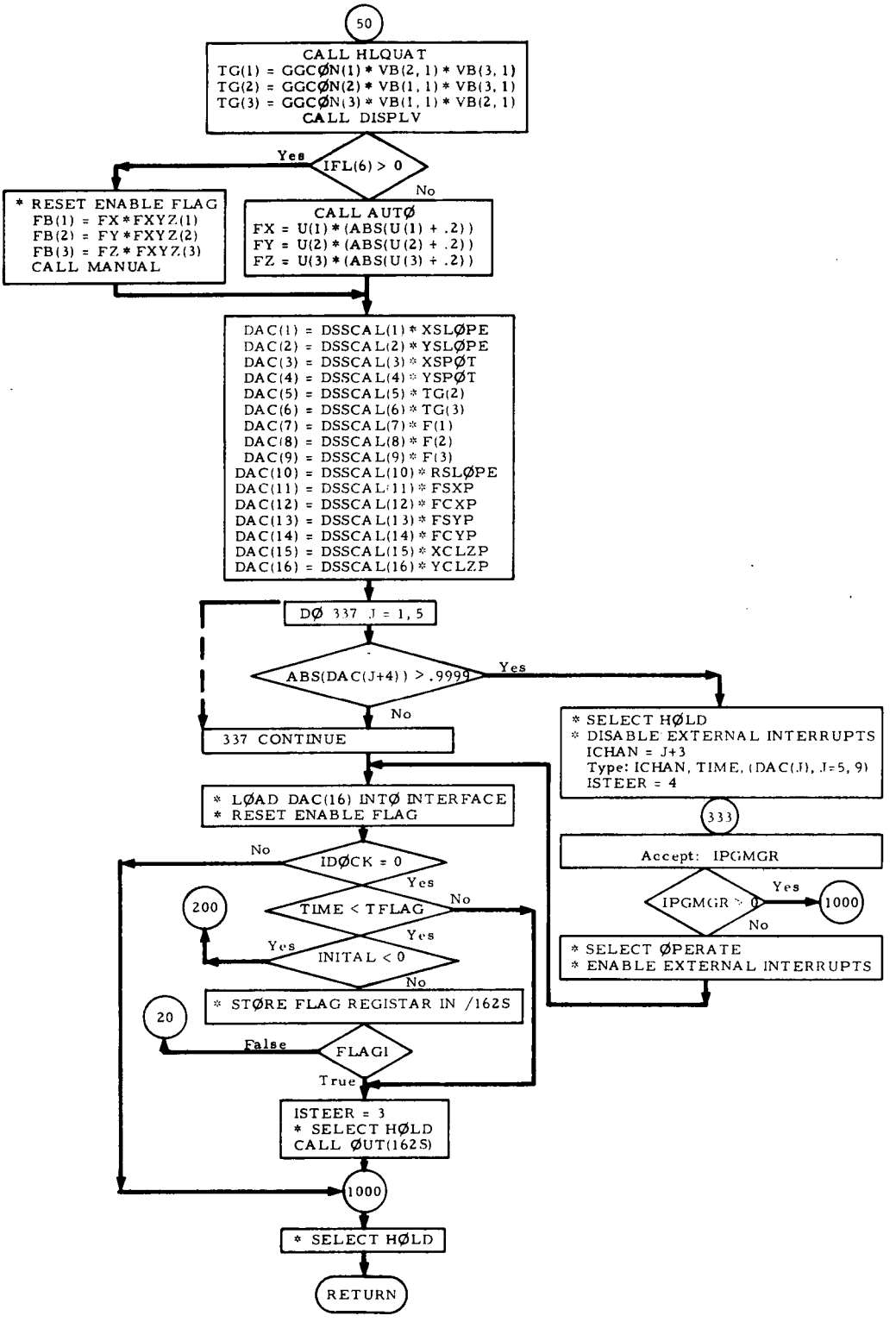

Fig. A-3 - (Concluded)

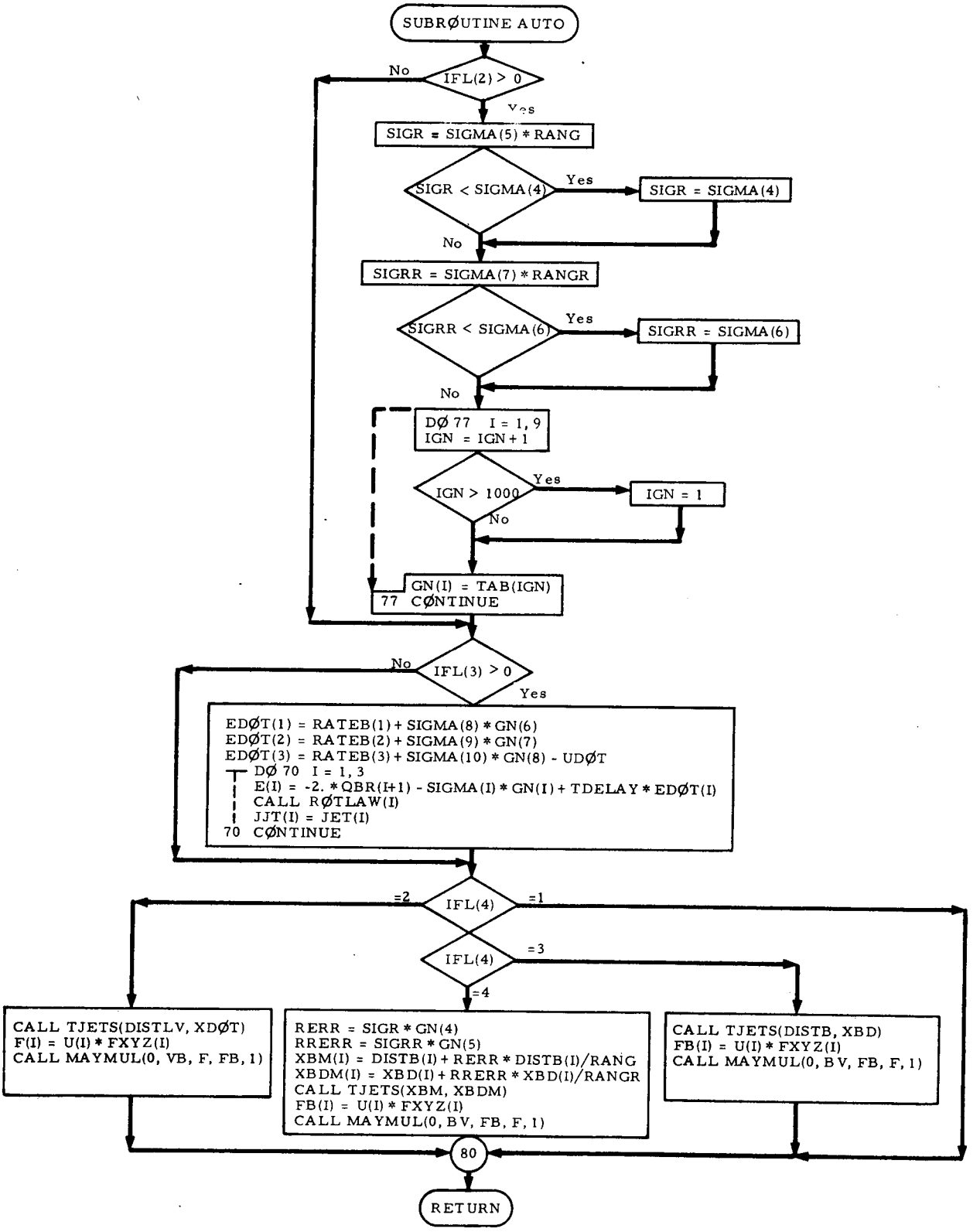

Fig. A-4 - Flow Chart of Subroutine AUTO

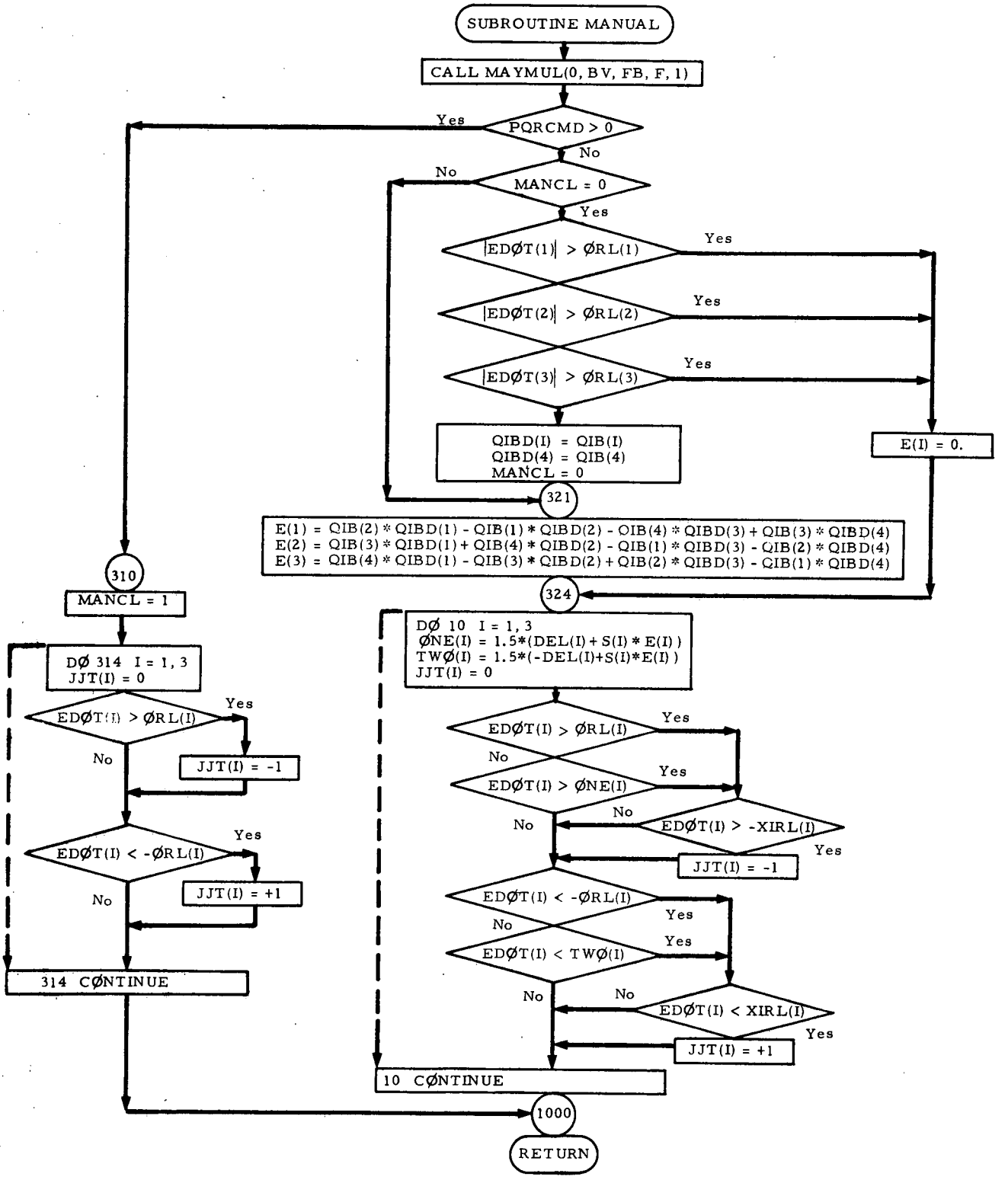

Fig. A-5 - Flow Chart of Subroutine Manual

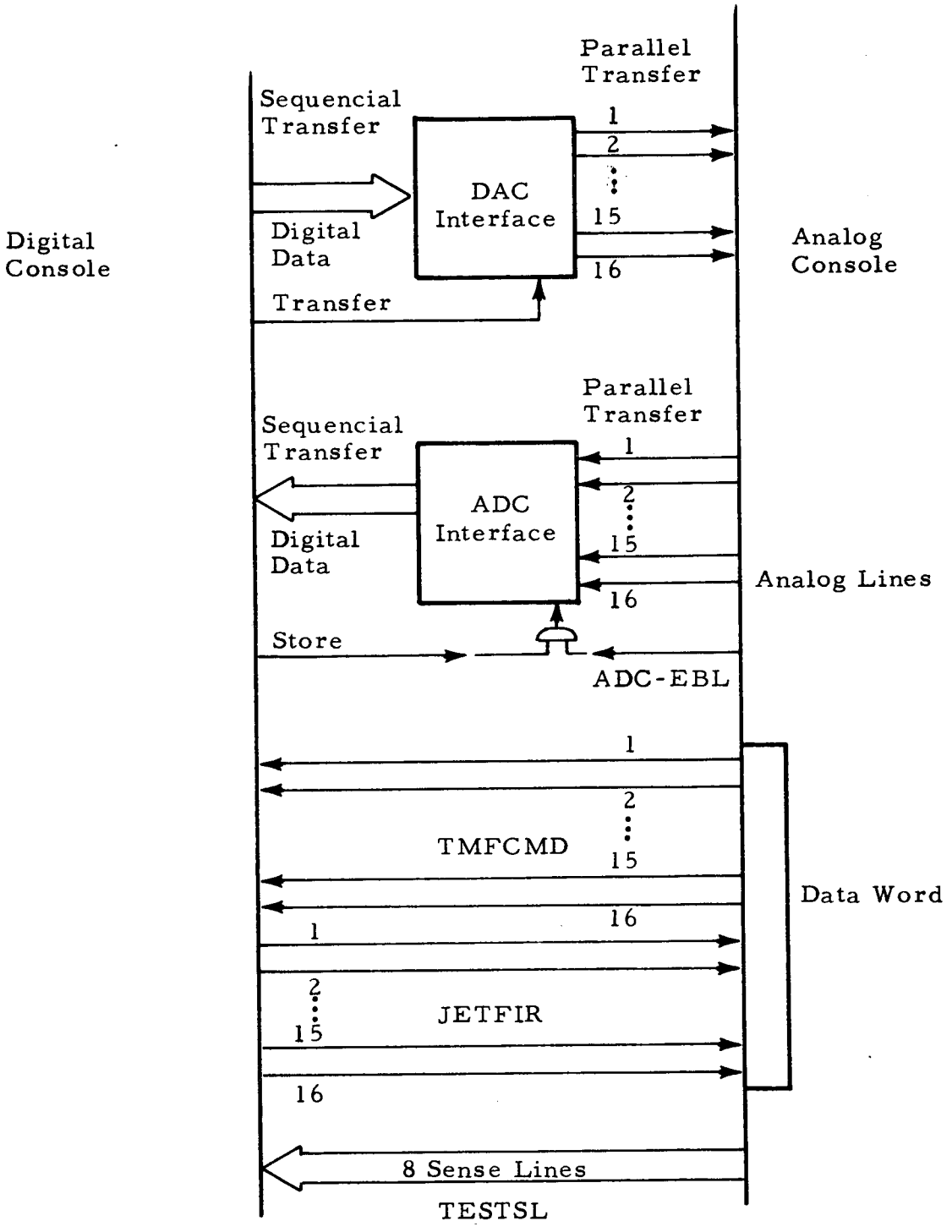

Fig. A-6 - Data Transfer During the Simulation

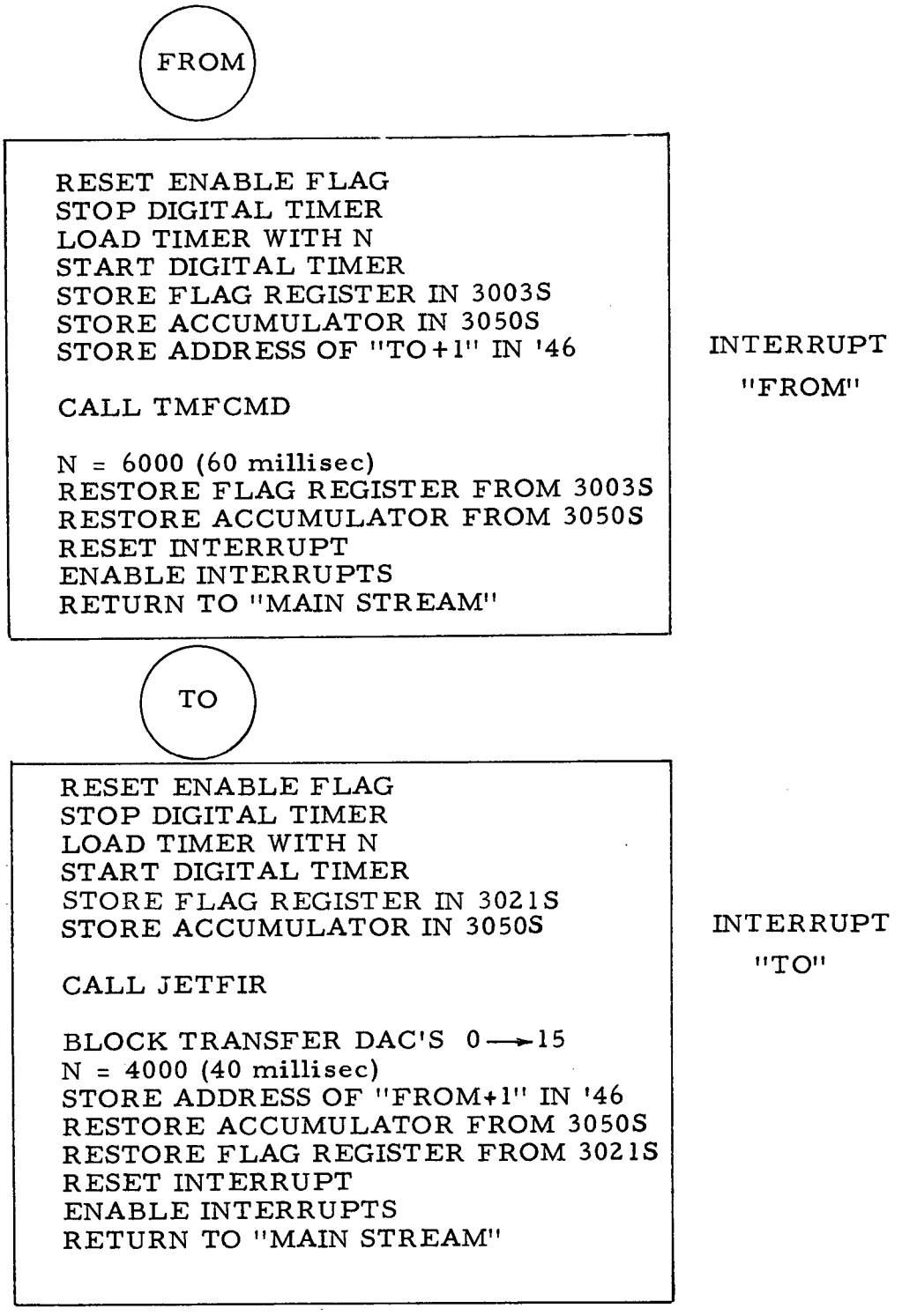

Fig. A-7 - Normal Timing Interrupts

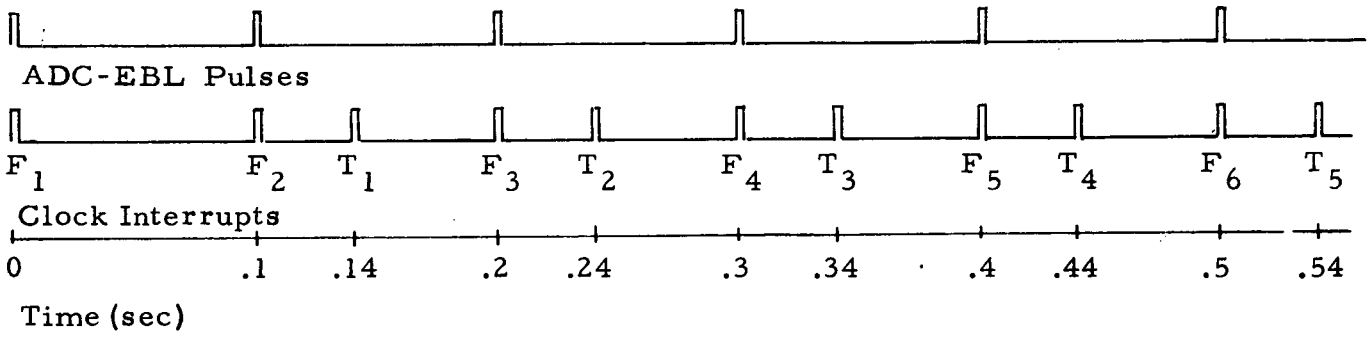

Fig. A-8 - Timing Sequence for the First 0.54 Seconds of Hybrid Simulation

Appendix B

ANALOG EQUATIONS AND WIRING DIAGRAMS

B-1

Appendix B

B.1 ANALOG EQUATIONS

The chaser equations of motion (translation, rotation, and kinematic) are shown below as they are solved on the analog computer. In these equations a dot over a variable indicates its time derivative (i.e., x = position, $\dot{x}$ = velocity, $\ddot{x}$ = acceleration). A quantity in brackets, $\left[\ \right]$, is a scaled analog term where 1.0 equals 100 volts.

Translation

$$\left[\frac{\ddot{x}(1)}{0.5}\right] = +200\omega \left[\frac{\dot{x}(2)}{50}\right] + 6000\omega^2 \left[\frac{x(1)}{1000}\right] + \frac{40{,}000}{M} \left[\frac{F(1)}{20{,}000}\right]$$

$$\left[\frac{\ddot{x}(2)}{0.5}\right] = -20\omega \left[\frac{\dot{x}(1)}{5}\right] + \frac{40{,}000}{M} \left[\frac{F(2)}{20{,}000}\right]$$

$$\left[\frac{\ddot{x}(3)}{0.5}\right] = -2000\omega^2 \left[\frac{x(3)}{1000}\right] + \frac{40{,}000}{M} \left[\frac{F(3)}{20{,}000}\right]$$

where,

- $x(i)$ = chaser position in local vertical coordinates (m)
- M = chaser mass (kg)
- ω = target orbital rate (rad/sec)
- $F(i)$ = control forces expressed in local vertical coordinates (N)

Rotation

Automatic Mode

$$\left[10\dot{P}\right] = -\left(\frac{I_{zz} - I_{yy}}{I_{xx}}\right)\left[100QR\right] + \left(\frac{10^{+6}}{I_{xx}}\right)\left[\frac{TC(1)}{10^{+5}}\right] + \left(\frac{4000}{I_{xx}}\right)\left[\frac{TG(1)}{40}\right]$$

$$\left[10\dot{Q}\right] = +\left(\frac{I_{zz} - I_{xx}}{I_{yy}}\right)\left[100PR\right] + \left(\frac{2\cdot10^{+6}}{I_{yy}}\right)\left[\frac{TC(2)}{2\cdot10^{+5}}\right] + \left(\frac{4000}{I_{yy}}\right)\left[\frac{TG(2)}{40}\right]$$

$$\left[10\dot{R}\right] = -\left(\frac{I_{yy} - I_{xx}}{I_{zz}}\right)\left[100PQ\right] + \left(\frac{2\cdot10^{+6}}{I_{zz}}\right)\left[\frac{TC(3)}{2\cdot10^{+5}}\right] + \left(\frac{4000}{I_{zz}}\right)\left[\frac{TG(3)}{40}\right]$$

Manual or Switching Mode

$$\left[10\dot{P}\right] = -\left(\frac{I_{zz} - I_{yy}}{I_{xx}}\right)\left[100QR\right] + \left\{LTC1+\right\}\left(\frac{10\,T_x}{I_{xx}}\right) - \left\{LTC1-\right\}\left(\frac{10\,T_x}{I_{xx}}\right)$$

$$\left[10\dot{Q}\right] = +\left(\frac{I_{zz} - I_{xx}}{I_{yy}}\right)\left[100PR\right] + \left(\frac{4000}{I_{yy}}\right)\left[\frac{TG(3)}{40}\right] + \left\{LTC2+\right\}\left(\frac{10\,T_y}{I_{yy}}\right) - \left\{LTC2-\right\}\left(\frac{10\,T_y}{I_{yy}}\right)$$

$$\left[10\dot{R}\right] = -\left(\frac{I_{yy} - I_{xx}}{I_{zz}}\right)\left[100PQ\right] + \left(\frac{4000}{I_{zz}}\right)\left[\frac{TG(3)}{40}\right] + \left\{LTC3+\right\}\left(\frac{10\,T_z}{I_{zz}}\right) - \left\{LTC3-\right\}\left(\frac{10\,T_z}{I_{zz}}\right)$$

$$\left[10\dot{E}(1)\right] = \left[10P\right] - \left\{LP+\right\}\left[10PC\right] + \left\{LP-\right\}\left[10PC\right]$$

$$\left[10\dot{E}(2)\right] = \left[10Q\right] - \left\{LQ+\right\}\left[10QC\right] + \left\{LQ-\right\}\left[10QC\right]$$

$$\left[10\dot{E}(3)\right] = \left[10R\right] - \left\{LR+\right\}\left[10RC\right] + \left\{LR-\right\}\left[10RC\right]$$

where

P, Q, R	=	angular rates about chaser body axes (rad/sec) (same as RATEB(i) defined in Appendix A)
PC, QC, RC	=	angular rate commands from pilot
I_{xx}, I_{yy}, I_{zz}	=	chaser principal moments of inertia (kg - m)
TC(i)	=	control torques about chaser body axes (N - m)
TG(i)	=	gravity gradient torques about chaser body axes (N - m)
T_x, T_y, T_z	=	absolute value of TC(i)
LTC1±, LTC2±, LTC3±	=	logical variables defined in Table B-1
LP±, LQ±, LR±	=	logical variables defined in Table B-2
$\dot{E}(i)$	=	chaser attitude rate errors (rad/sec).

Illegal combinations of logical variables are prevented from occurring. Illegal sets are those which require opposing jets to fire and result in no net thrust (i.e., LTC1+ = LTC1- = 1, LP+ = LP- = 1, etc).

Kinematics

$$\left[10\ \dot{\overline{QIB(1)}}\right] = -\left[5P\ \overline{QIB(2)}\right] - \left[5Q\ \overline{QIB(3)}\right] - \left[5R\ \overline{QIB(4)}\right]$$

$$\left[10\ \dot{\overline{QIB(2)}}\right] = +\left[5P\ \overline{QIB(1)}\right] - \left[5Q\ \overline{QIB(4)}\right] + \left[5R\ \overline{QIB(3)}\right]$$

$$\left[10\ \dot{\overline{QIB(3)}}\right] = +\left[5P\ \overline{QIB(4)}\right] + \left[5Q\ \overline{QIB(1)}\right] - \left[5R\ \overline{QIB(2)}\right]$$

$$\left[10\ \dot{\overline{QIB(4)}}\right] = -\left[5P\ \overline{QIB(3)}\right] + \left[5Q\ \overline{QIB(2)}\right] + \left[5R\ \overline{QIB(1)}\right]$$

$$\left[\frac{\overline{QIB(i)}}{2}\right] = \left[\frac{1}{2\sqrt{QIB(1)^2 + QIB(2)^2 + QIB(3)^2 + QIB(4)^2}}\right] \left[QIB(i)\right] \quad i=1,2,3,4$$

where,

QIB(i) = quaternions relating inertial coordinates to chaser body coordinates

$\overline{QIB(i)}$ = orthogonalized QIB(4)

Table B-1

LOGICAL VARIABLES FROM DATA WORD WHICH REPRESENT ATTITUDE THRUSTER FIRINGS

LTC1+ = 1,0 (logical)	for positive attitude thrust	(P channel)
LTC1- = 1,0	negative	(P channel)
LTC2+ = 1,0	positive	(Q channel)
LTC2- = 1,0	negative	(Q channel)
LTC3+ = 1,0	positive	(R channel)
LTC3- = 1,0 (logical)	for negative attitude thrust	(R channel)

Table B-2

LOGICAL VARIABLES WHICH REPRESENT RATE COMMANDS FROM THE PILOT

LP+ = 1,0 (logical)	for positive rate command	(P channel)
LP- = 1,0	negative	(P channel)
LQ+ = 1,0	positive	(Q channel)
LQ- = 1,0	negative	(Q channel)
LR+ = 1,0	positive	(R channel)
LR- = 1,0 (logical)	for negative rate command	(R channel)

B.2 ANALOG WIRING DIAGRAMS

Symbols used in the analog wiring diagrams are defined in Fig. B-1. Diagrams of the translation, rotation, and kinematic equations are shown in Figs. B-2, B-3, and B-4, respectively.

In Fig. B-2 the analog switches SW001, SW011, SW021, and SW031 are switched left (L), facing the panel, to decouple the translation equations and they are switched right (R) to add cross coupling. Control line 1 (CL1) is used to scale up the analog position values for improved accuracy when all three axes are less than 45 meters.

The manual command logic is shown in Fig. B-5; display logic is shown in Fig. B-6, and timing logic is shown in Fig. B-7.

B.3 AUTOMATIC ANALOG SET-UP

A hybrid program is used during set-up of the simulation. This program calculates the analog potentiometer values and automatically sets the potentiometers. It also provides the operator with a check list of required setup procedures. A listing of this program is presented in Fig. B-8. Standard symbols are used where possible. Other symbols not previously defined are:

W1 = ω
W2 = ω^2
J1 = label of a fixed value
C002 = address of potentiometer No. 002.

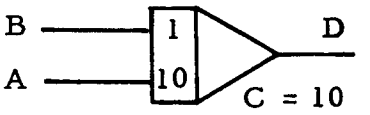

Integrator

$$D = \frac{-1}{C} * \int (1*B + 10*A)\,dt$$

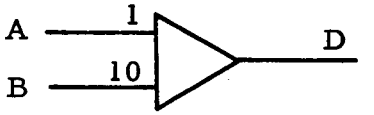

Summer

$$D = -(1*A + 10*B)$$

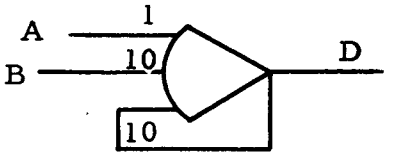

High Gain

$$D = \frac{-1}{10} * (1*A + 10*B)$$

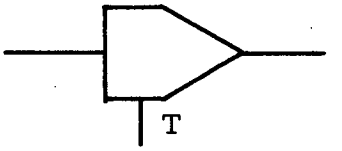

Track and Store

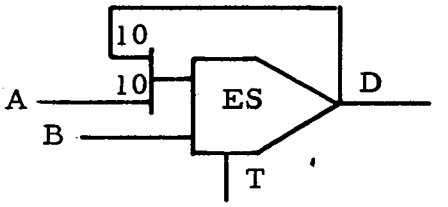

Electronic Switch

D = -A if T = 1 (logical)
D = -B if T = 0 (logical)

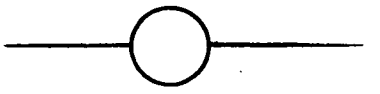

Potentiometer

Digital Control Line 6

Fig. B-1 - Symbols Used in Wiring Diagrams

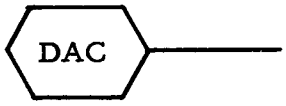

Digital-to-Analog Converter Output

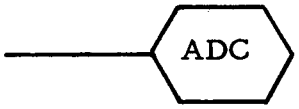

Analog-to-Digital Converter Input

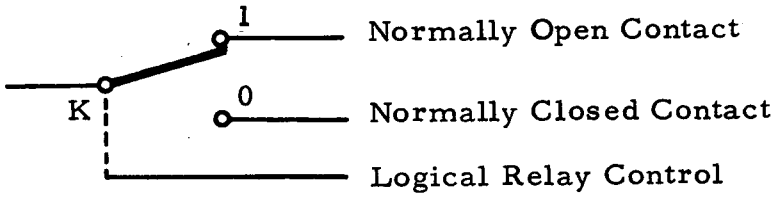

Relay

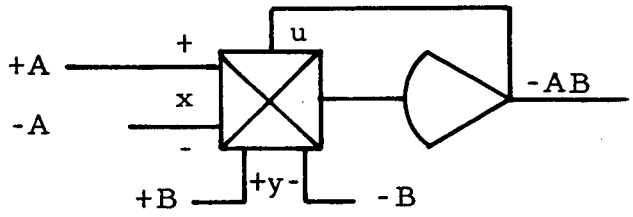

Multiplier

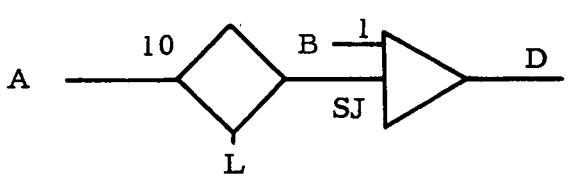

D = -1.0 * B if L = 0 (logical)

D = -1.0*B - 10*A if L = 1 (logical)

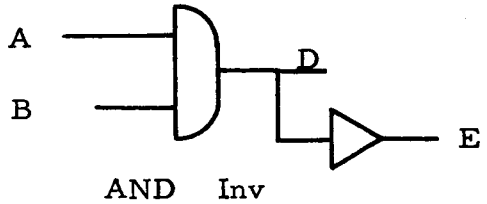

AND Inv

$D = A \cdot B$

$E = \overline{A \cdot B}$

Fig. B-1 - (Continued)

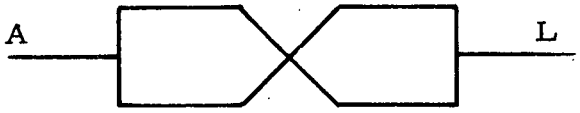

Logic Trunk

L = 1 if A > 0 volts
L = 0 if A $\leq$ 0 volts

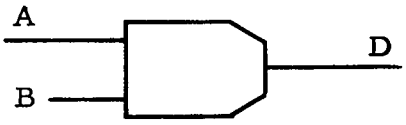

Comparator

D = 1 if (A + B) > 0 volts
D = 0 if (A + B) $\leq$ 0 volts

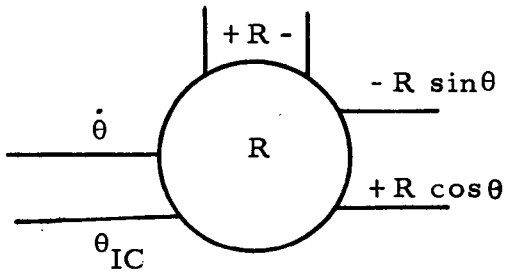

Resolver

Fig. B-1 - (Concluded)

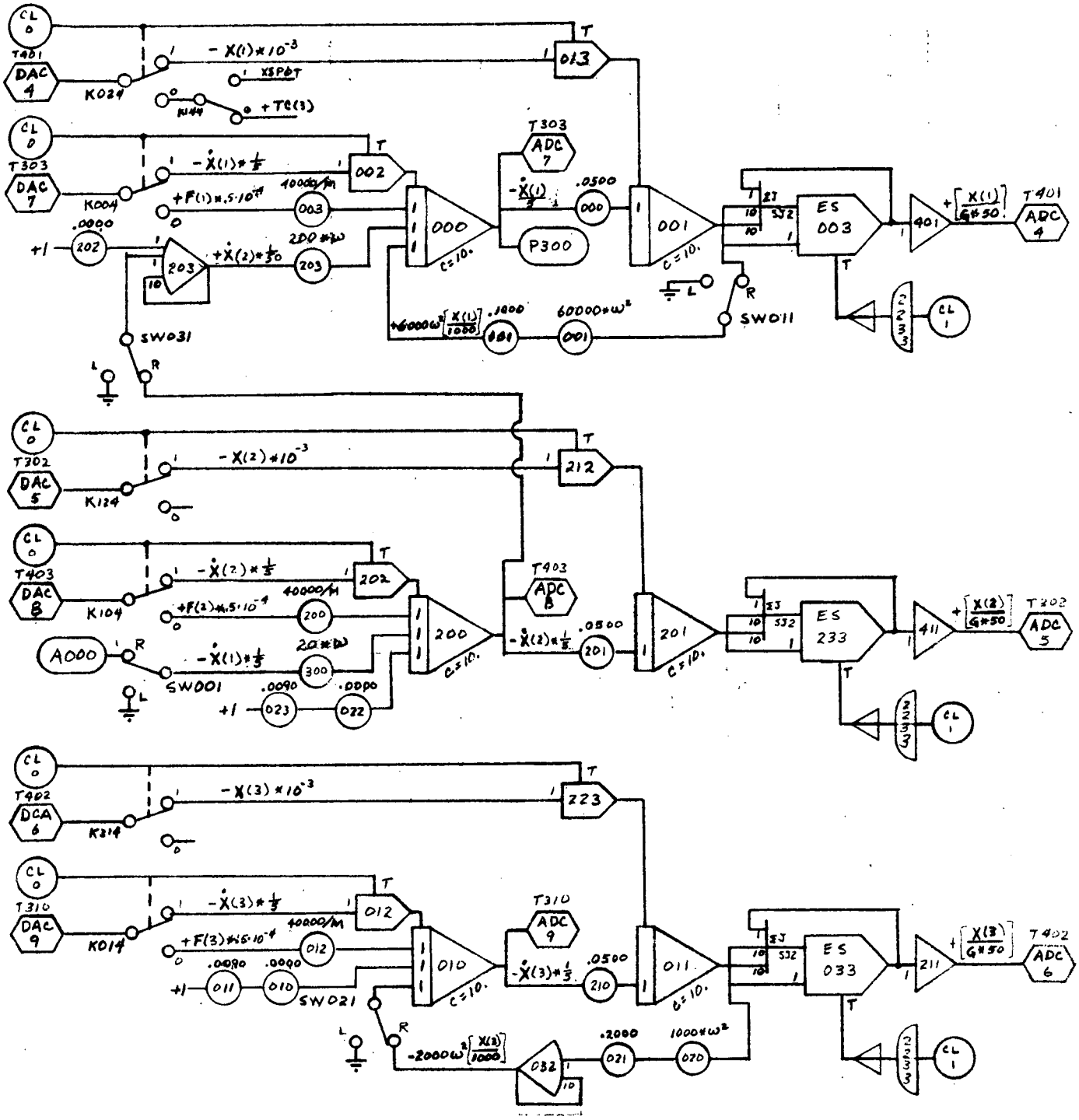

Fig. B-2 - Analog Wiring Diagram for Chaser Translation

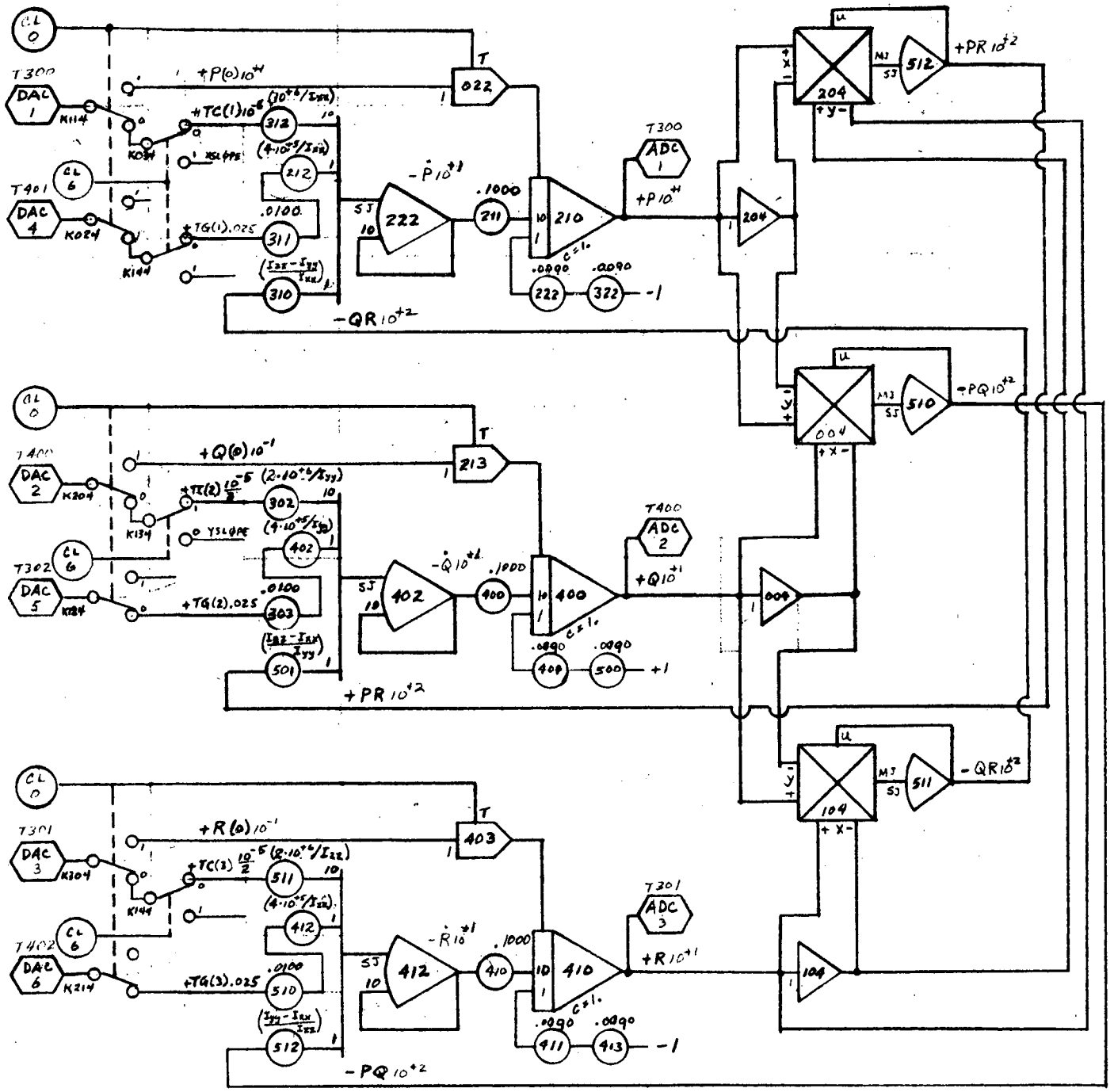

Fig. B-3 - Analog Wiring Diagram for Chaser Rotation

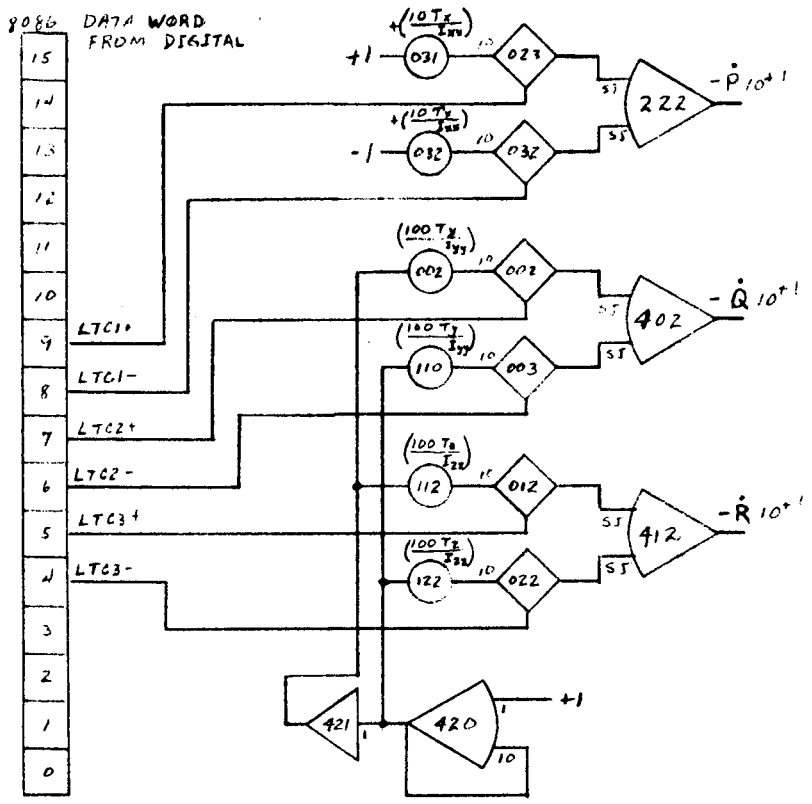

Fig. B-3 - Concluded

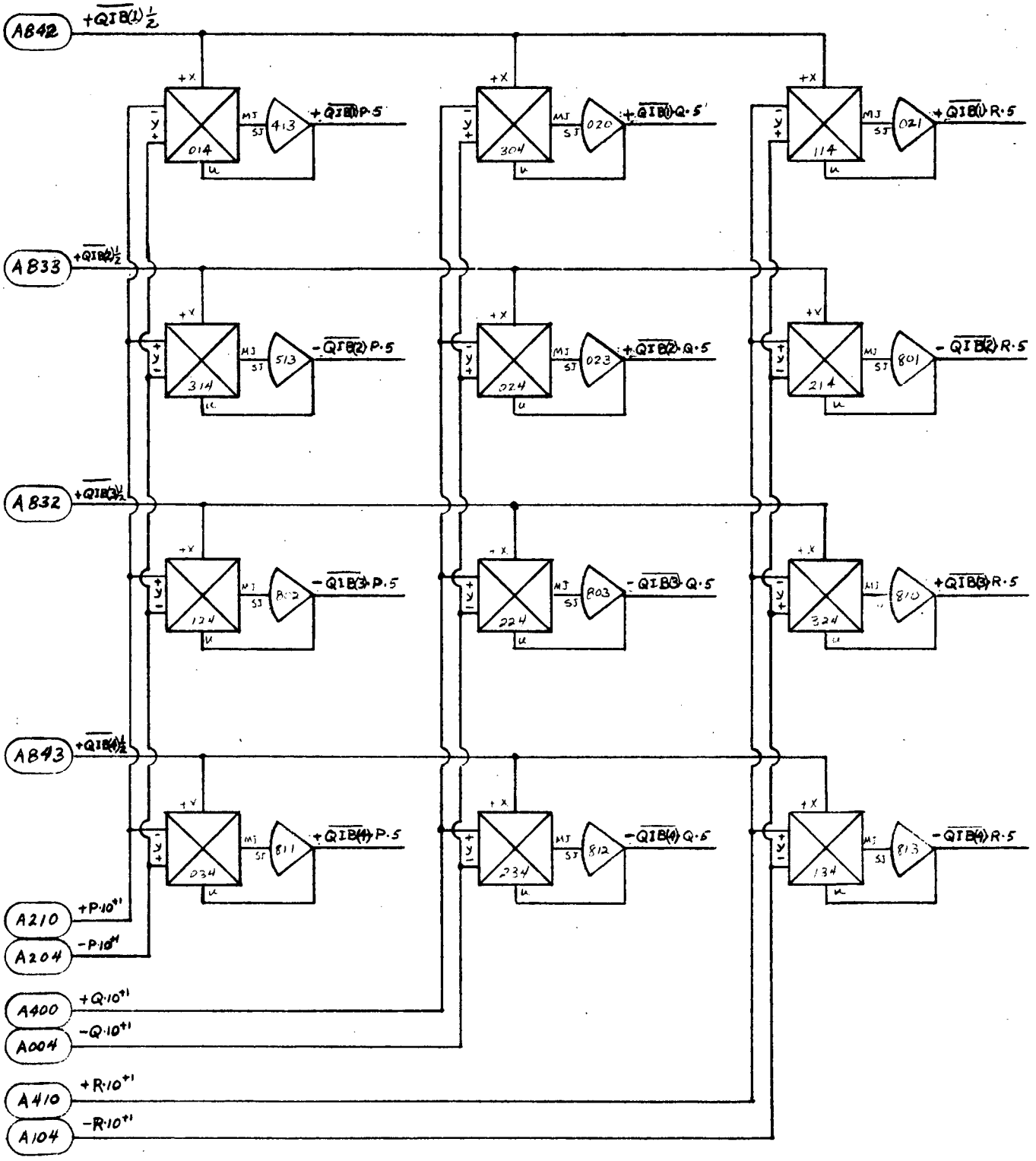

Fig. B-4 - Analog Wiring Diagram for Chaser Attitude

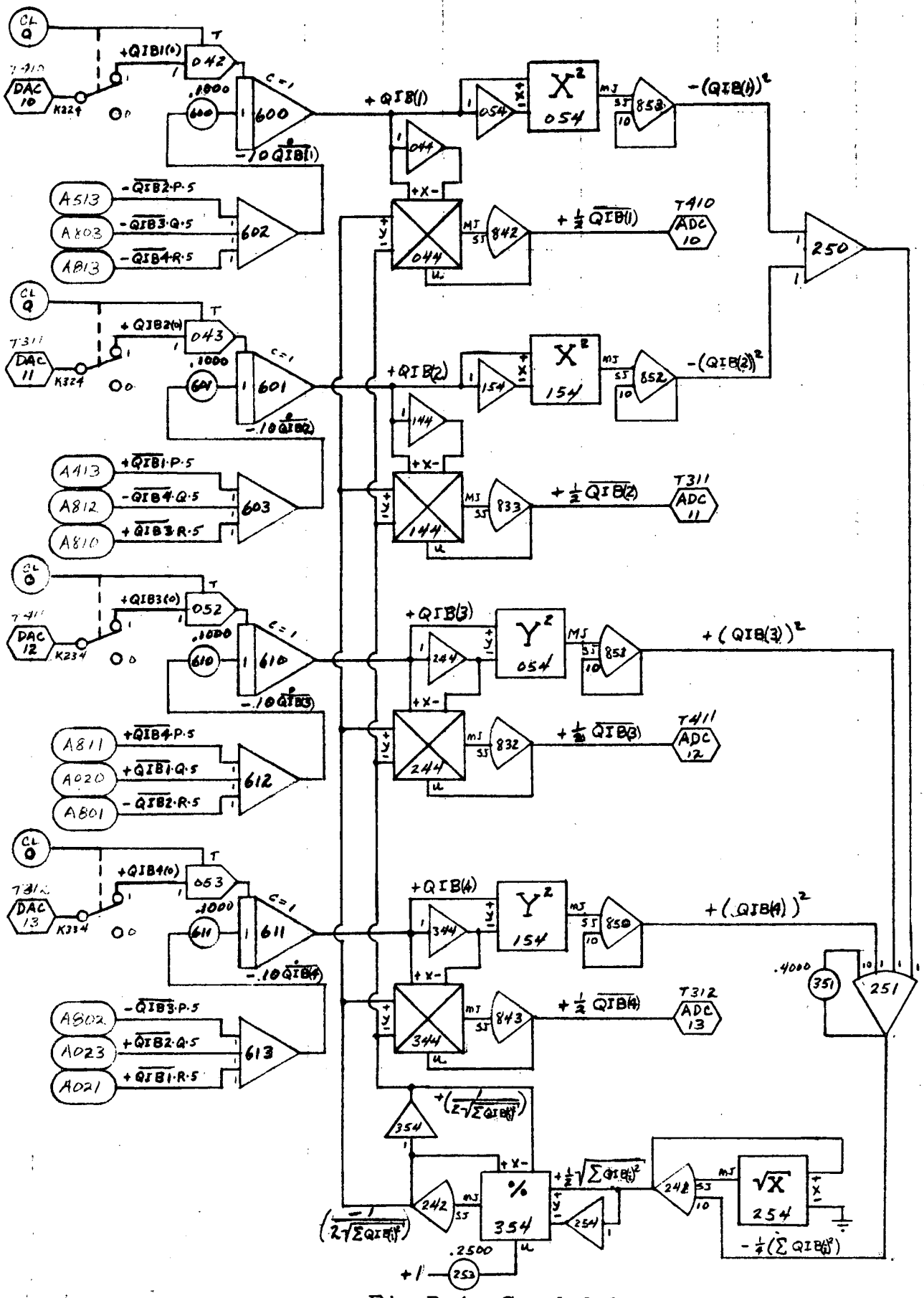

Fig. B-4 - Concluded

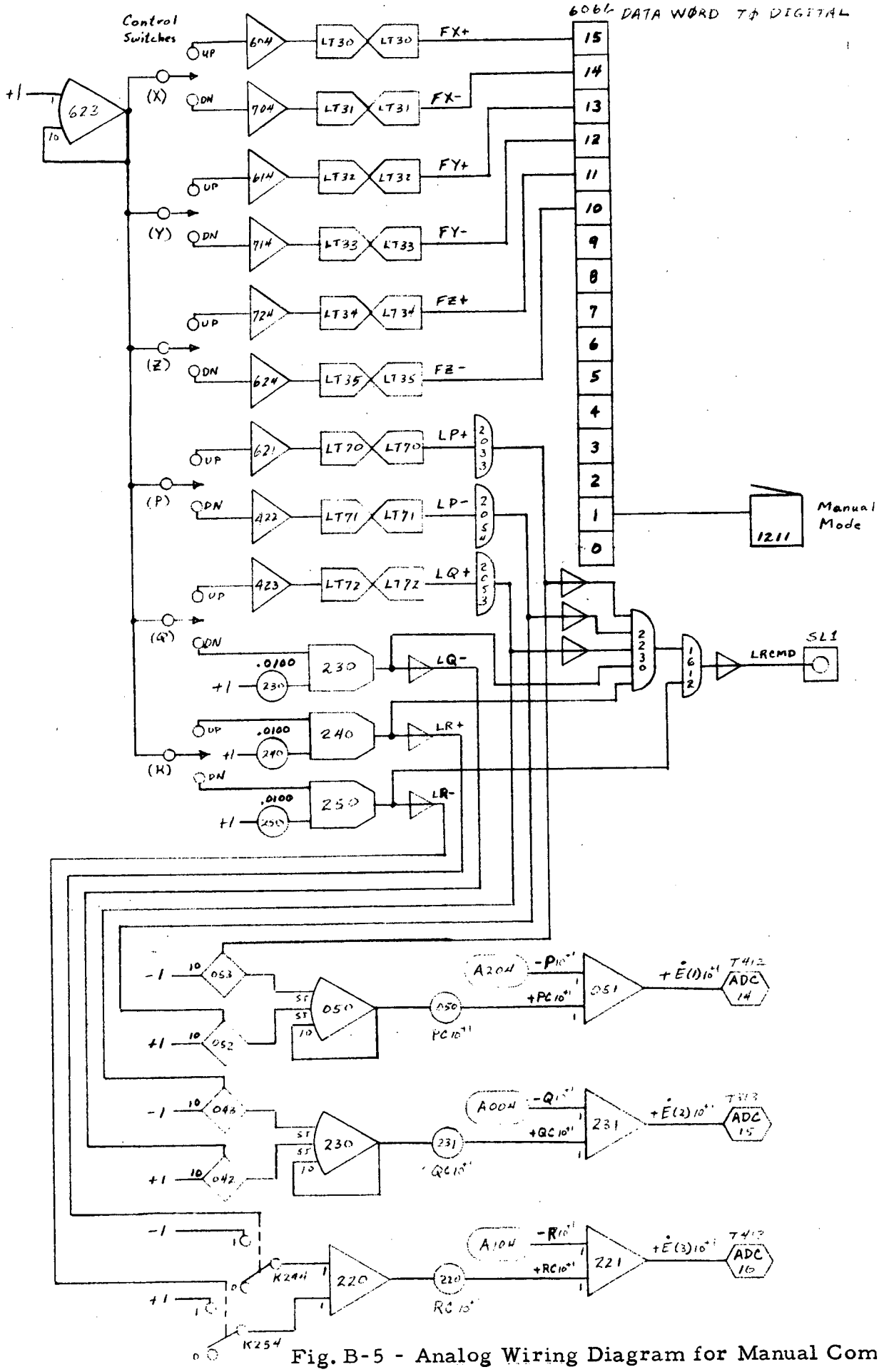

Fig. B-5 - Analog Wiring Diagram for Manual Commands

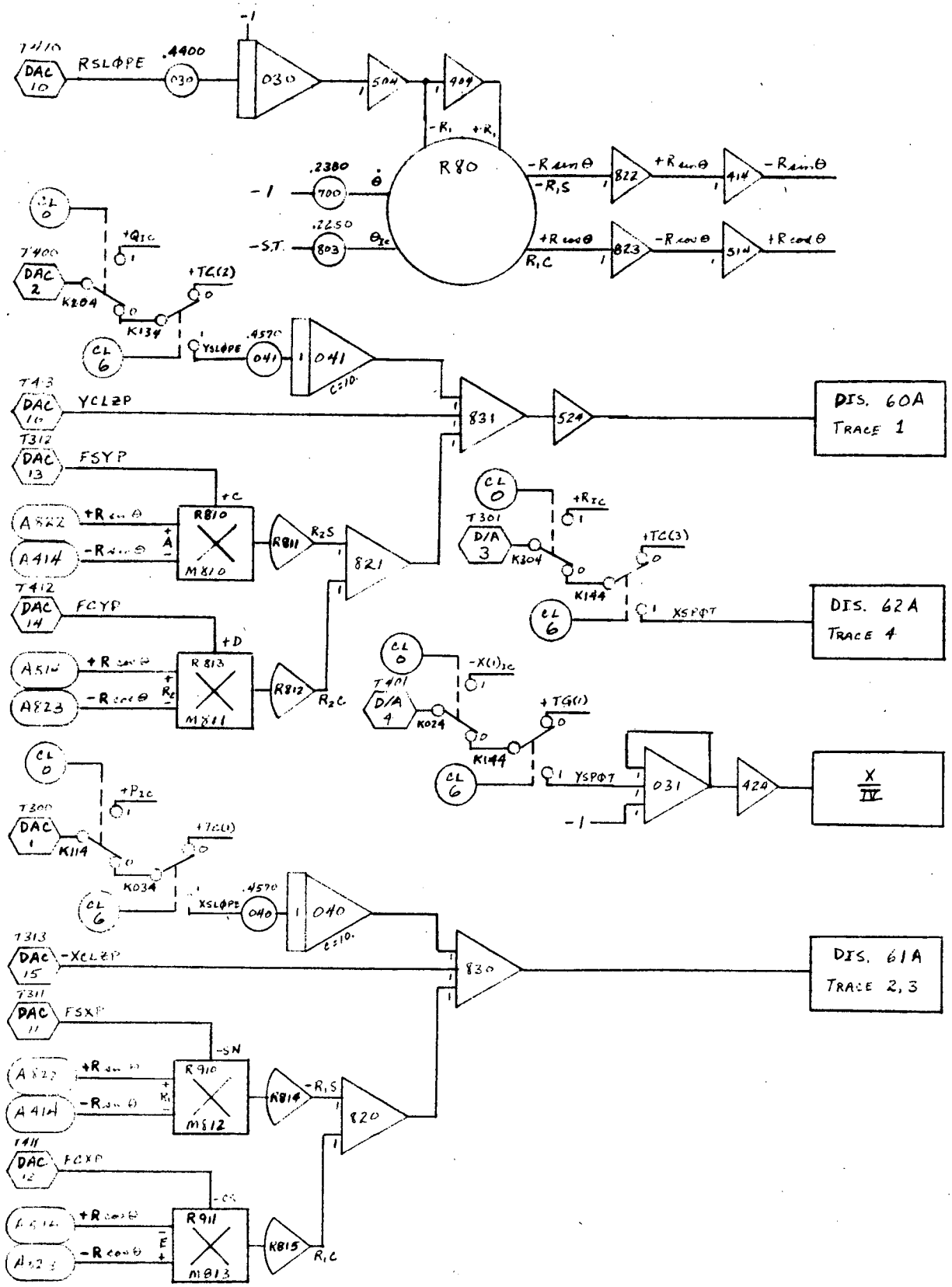

Fig. B-6 - Analog Wiring Diagram for Display Generation

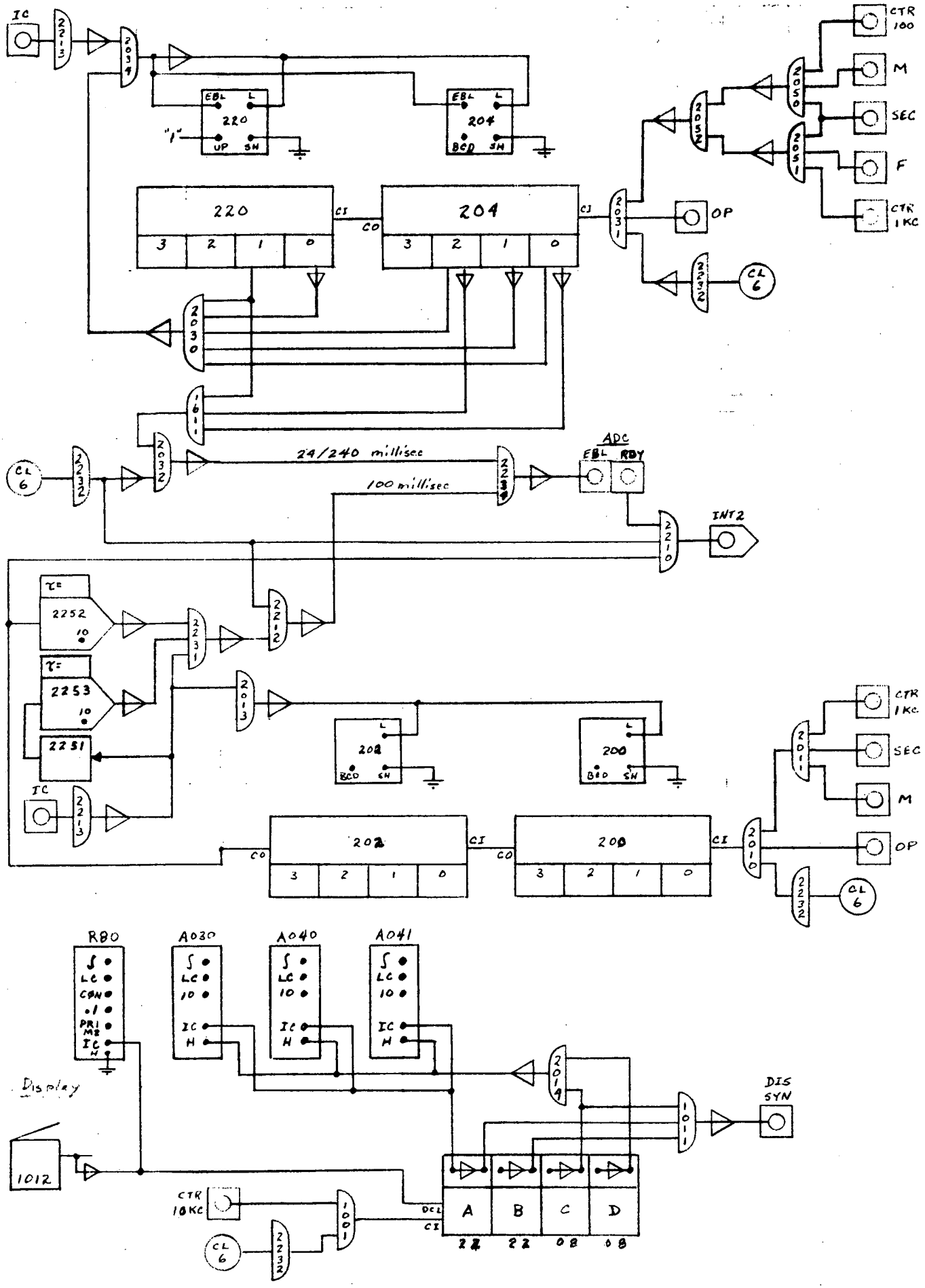

Fig. B-7 -Analog Wiring Diagram of Timing Logic

```
$JOB  H-10      HEESCHEN       N8-5C99-1003          2/1/72
$HOI,,IU1,
          JCE,XMODE;    ▲CONTINUE-ON-ERROR OPTION▲
          1,CONSOLE;
          JPS,MODE;
          ▲SPACE SHUTTLE DOCKING STUDY▲;;  ▲MKS▲;
          ▲SET DIGITAL TIMER;    RED:RED▲;
          ▲SET ANALOG TIMER;     A=22, B=22, C=08, D=08▲;
          ▲SET DFG'S TO INV.▲;
          JS,JT,INPUT;▲ARE DAC'S OUT OF LOOP TEST?▲;▲TYPE GO▲;
 1.0100)  ▲INPUT DATA▲
 1.0110)  BC=.0090,B0=.0000,
 1.0200)  W1=1.106773E-3,    W2=1.2249465E-6,
 1.0300)  M = 1.264426E+5,
 1.0310)  TX = 2.7116E+4,
 1.0320)  TY = 5.7622E+4,
 1.0330)  TZ = 5.0842E+4,
 1.0400)  IXX = 4.2030E+6,
 1.0500)  IYY = 2.0520E+7,
 1.0600)  IZZ = 2.3190E+7,
 1.0610)  PC=.3500,QC=.3500,RC=.3500,
 1.0700)  J1=.0100,J2=.1000,J3=.2500,J4=.4000,J5=.0500,J6=.8300,
 1.0710)  J7=.4400,J8=.2380,J9=.4570,J10=.2000,
 1.0720)  ▲COEFFICIENT CALCULATION▲
 1.0800)  C000=J5,C001=6.E+4*W2,C003=40000./M,C010=B0,C011=BC,
 1.0810)  C002=(100.*TY)/IYY,C030=J7,C031=(10.*TX)/IXX,C032=(10.*TX)/IXX,
 1.0900)  C020=1000.*W2,C021=J10,C022=B0,C023=BC,C101=J2,
 1.0910)  C110=(100.*TY)/IYY,C112=(100.*TZ)/IZZ,C122=(100.*TZ)/IZZ,
 1.1000)  C200=40000./M,  C201=J5,C202=B0,C203=200.*W1,C210=J5,C211=J2,
 1.1100)  C212=4.E+5/IXX,C222=B0,C253=J3,C300=20.*W1,C302=2.E+6/IYY,
 1.1110)  C230=J1,C240=J1,C250=J1,     C012=40000./M,
 1.1120)  C050=PC,C220=RC,C231=QC,
 1.1200)  C303=J1,C310=(IZZ-IYY)/IXX,C311=J1,C312=1.E+6/IXX,C322=BC,
 1.1300)  C351=J4,C400=J2,C401=B0,C402=4.E+5/IYY,C410=J2,C411=B0,
 1.1400)  C412=4.E+5/IZZ,C413=BC,C500=BC,C501=(IZZ-IXX)/IYY,C510=J1,
 1.1500)  C511=2.E+6/IZZ,C512=(IYY-IXX)/IZZ,C600=J2,C601=J2,C610=J2,
 1.1600)  C611=J2,C700=J8,C040=J9,C041=J9,
          JD,JL,OUTPUT;
          1;       ▲LIST PROGRAM▲
          1;       ▲EXECUTE PROGRAM▲
          $COEF:   ▲LIST COEFFICIENTS▲
          JS,JT,OUTPUT;
          JPS,MODE;$COEF,SET;  ▲ALL POTS SET▲;
          JS,JT,INPUT;  ▲PAUSE TO CORRECT POTS▲;▲TYPE GO▲;
          .0004,VERIFY;$COEF,READ;  ▲ALL POTS CHECKED▲;
          NORMAL;
          JCL00,0,SET;
          JCL01,0,SET;
          JCL06,1,SET;
          JS,JT,INPUT;▲TYPE GO▲;
           3,CONSOLE;        ▲EXIT PROGRAM▲
$JOB
$RW,,SU1
```

Fig. B-8 - Listing of Hybrid Set-up Routine